IWMI International Water Management Institute

igrac International Groundwater Resources Assessment Centre

USAID FROM THE AMERICAN PEOPLE

Assessing the feasibility of Managed Aquifer Recharge in Ramotswa Transboundary Aquifer Area

December 2018

Submitted by:

Implemented by:

In partnership with:

This report was made possible by the support of the American people through the United States Agency for International Development (USAID). Its contents are the sole responsibility of IWMI, and do not necessarily reflect the views of USAID or the United States Government.

Contributors
Girma Y. Ebrahim (IWMI)
Simon Trust (IWMI)
Manuel Magombeyi (IWMI)
Karen G. Villholth (IWMI)
Jonathan Lautze (IWMI)
Geert-Jan Nijsten (IGRAC)
Keetile Keodumetse (DWA-Botswana)
Piet Kenabatho (University of Botswana)
Sakhile Mndaweni (DWS - South Africa)
Moses Moehadu (WUC, Botswana)
Modreck Gomo (University of Free State –South Africa)
Bochengedu Somolekae (DWA-Botswana)
Charles Nkile (DWA-Botswana)

Acknowledgments
The contribution and support from the Department of Water and Sanitation (DWS) – South Africa, The Department of Water Affairs (DWA) - Botswana, Botswana Geoscience Institute (BGI) – Botswana, and the Water Utilities Corporation (WUC) – Botswana is acknowledge.

Executive Summary

Improving water security Improving water security is essential to assuring satisfaction of water demand in the face of increasing population, droughts, and climate variability and change. Managed Aquifer Recharge (MAR) is one means for achieving water security. MAR is the purposeful recharge of water into the aquifer at times where there is excess and for subsequent recovery when demand is high. MAR has been identified in many places as both a practical and necessary strategy for achieving water-recycling goals and achieving water security. Application of MAR is becoming increasingly important, particularly in semi-arid and arid regions where recharge is very low and evaporation is very high. MAR has advantages over surface storage in dams/ reservoirs such as reduced land use, reduced loss of evaporation. However, MAR has to be designed and implemented very carefully, as it may not be feasible at all sites due to various constraints such as hydrogeological, water source availability, water quality, and cost limitations. Various hydrogeological factor limit application of MAR. Degradation of water quality due to physical, chemical or biological processes and change in water quality due to mixing of recharge water with native groundwater is another concern in the application of MAR. MAR in karstic aquifer is even more challenging due to vulnerability of the aquifer to contamination and Presence of high permeability preferential flow zones resulting losses of stored water.

Report objective the main objective of this report is to assess the technical feasibility of MAR in the Ramotswa Transboundary Aquifer Area using the hydrogeological model. It also includes identifying possible MAR sites, identifying contaminants of concern in karstic aquifer through literature review, assessing water source availability and water quality and evaluating geochemical implication of mixing of recharge water and native groundwater

Approach A hydrogeological modelling approach was used to investigate the feasibility of MAR in the Ramotswa Transboundary aquifer. The modelling framework involves a simulation-optimization approach. A transient 3D hydrogeological model (described in the complementary hydrogeological modelling deliverable) was used with a past Groundwater Management model (2005) to estimate aquifer storage potential during very wet year (2009) and dry year (2017). Optimization involves maximization of groundwater recharge during the three month period [January – March] given groundwater level constraint. The three month recharge period was chosen based on long-term rainfall data. The selected MAR method is the infiltration basin method, which is probably the most common and affordable MAR method. Soil infiltration tests conducted during this study were used to determine the upper limit of infiltration from the recharge basins. Particle tracking simulations were performed using MODPATH to evaluate the residence time of infiltrated water before it is recovered by existing production boreholes. Water quality characterization was carried out based on surface and groundwater quality data available for the study area. Geochemical reaction of concerns and risks (mixing of recharge water with native groundwater) identified during the literature review were assessed using a Geochemical Model. Water source for MAR are identified. Quantitative estimates of available wastewater is made based on population data, per capita consumption and assumed percentage connection to the sewer network connection.

Results. The total volume of water that can be injected into the aquifer in three months period [Jan-March] during the dry period in Botswana is 1920 m^3/d (**0.172 x 10^6 m^3**) and in South Africa is 6540 m^3/d (**0.589 x 10^6 m^3).** During the wet period recharge volume is reduced due water level increase

that results in less available storage space. The total volume of water recharged during the wet period is 741 m^3/d (**0.067 x 10^6 m^3**) in Botswana and 4600 m^3/d (**0.414 x 10^6 m^3)** in South Africa. Results of particle tracking show that none of the production borehole capture injected water less than 60 days old, as regulatory limit required for inactivation of pathogens or other nutrients commonly present in treated wastewater. The water quality characterization results shows high spatial variability in water quality. High Nitrate is the other problem which highly recognized problem in the area. However, since the selected MAR sites are far from the village area, MAR operation is less affected. The geochemical modelling results shows no further dolomite dissolution due to MAR in particular when the recharge water is alkaline. However, as already observed in the Ramotswa production boreholes the issue of iron incrustation (clogging) still be a problem. Water budget and water level analysis after three month recharge period has shown that there is little scope for the stored water to stay in the aquifer for subsequent recovery during the dry period. It is important to note that due to shallow depth to groundwater the stored water is lost through evapotranspiration directly from the groundwater. In this case immediate pumping, after recharge (e.g. April, within one month after recharge) would be needed to optimize recharge water.

Conclusions Due to shallow depth to groundwater and high evapotranspiration from groundwater, conditions seems less favourable to store water unless short-term storage is desired. It is important to note that estimated evapotranspiration may be high due to uncertainty in the extinction depth used in the hydrogeological model.

Table of Contents

List of Figures

List of Tables

Acronyms

amsl	Above Mean Sea Level
AET	actual evapotranspiration
BGI	Botswana Geoscience Institute
DEM	Digital Elevation Model.
DWA	Department of Water Affairs (Botswana)
DWS	Department of Water and Sanitation (South Africa)
ET	Evapotranspiration
GWET	Groundwater Evapotranspiration
IGRAC	International Groundwater Resources Assessment Centre
IWMI	International Water Management Institute
LULC-	Land Use Land Cover
MAR	Managed Aquifer Recharge
mbgl	metres below ground level
ModelMuse	Graphic user interface for MODFLOW-2005, MODFLOW-OWHM, and others
MODFLOW	Modular Three-Dimensional Finite-Difference Groundwater Flow Model
SRTM	Shuttle Radar Topography Mission
SWL	Static Water Level
USDA	United States Department of Agriculture
USAID	United States Agency for International Development
USGS	U.S. Geological survey
WLE	Water, Land and Ecosystems
WUC	Water Utilities Corporation (Botswana)

1. Introduction

1.1 Background

Groundwater is the main water source in the Ramotswa Transboundary Aquifer Area (RTBAA). An imbalance between groundwater recharge and abstraction caused groundwater levels in the area to decline in recent years. In response, the concept of groundwater replenishment using Managed Aquifer Recharge (MAR) is investigated in this project. MAR has been practiced in many areas as a means of increasing groundwater availability and improving the overall reliability of water supplies. Storing water in an aquifer during times of excess supply and recovering the same water for use when the demand is high is becoming an attractive water management option. This has certain advantages over surface storage in dams such as reduced land use, reduced loss of evaporation. Hydrogeological models can be used to assess the feasibility of MAR prior to conducting expensive field test. They provide important information such as storage capacity of the aquifer, the response of the aquifer to induced recharge, location of recharge and recovery, and recovery efficiency (Mansouri and Mezouary, 2015; Woolfenden and Koczot, 2001). Hydrogeological models have been used in the past to assess the feasibility of MAR in combination with field experiments (Flint and Ellett, 2004; Ganot et al., 2017; Hsieh et al., 2010; Izbicki et al., 2008; Xu et al., 2017). Some studies combined hydrogeological model with optimization algorithms to assess the feasibility of MAR (Ebrahim et al., 2015; Jonoski et al., 1997). Importantly, feasibility assessment of MAR should consider source water availability for recharge, water quality of source water and recharge water, geochemical implication of mixing of recharge water and water demand.

1.2 Objectives

The **main objectives** of this study is to assess the technical feasibility of MAR in the RTBAA, using the hydrogeological model

The specific modeling objectives include:

- characterizing water quality in Ramotswa aquifer
- identifying contaminant of concerns in the karst aquifer through literature review
- assessing water source availability for MAR
- evaluating the geochemical implication of mixing of recharge water with native groundwater using geochemical modeling
- identifying suitable sites for MAR application and scenario analysis
- determining storage capacity of the aquifer using hydrogeological model
- investigating water level response to induced recharge such as building up of groundwater level (mound),
- determining residence/travel time of recharged water before recovered by existing production wells. To confirm that the sufficient residence time for contaminant attenuation in recharge water

2. Description of the study area

2.1 Ramotswa Transboundary Aquifer Area

Ramotswa Transboundary Aquifer Area (RTBAA) The Ramotswa Aquifer is located in the Upper Limpopo River Basin encompasses an aquifer shared between South Africa and Botswana. The Ramotswa Aquifer corresponds to the Ramotswa dolomitic aquifer extent mapped based on surface geology. The RTBAA is a slightly broader term than the strict boundary. RTBAA is used to capture areas in the subsurface that are hydrologically linked to the aquifer, but which lie outside the dolomitic aquifer boundaries delineated based solely on surface geology (Figure 1).

Ramotswa Aquifer Flight Area The flight area (area about 1,500 km^2) was commonly used as an encompassing boundary within which the aquifer was found. It was used to overcome ambiguities of a precise boundary for the aquifer in phase 1 of the RAMOTSWA project. Airborne geophysical surveys were indeed conducted within this flight area in 2016 (Figure 1).

Gaborone Dam Catchment The Gaborone catchment area, located in the Upper Limpopo River Basin (Area ~4,318 km^2, Figure 1), reflects the immediate surface water boundaries within which the Ramotswa Aquifer is located. Given the linkages between surface and groundwater, the catchment is a very relevant scale. Phase 2 of the RAMOTSWA project treats the Gaborone Dam Catchment as its project study area.

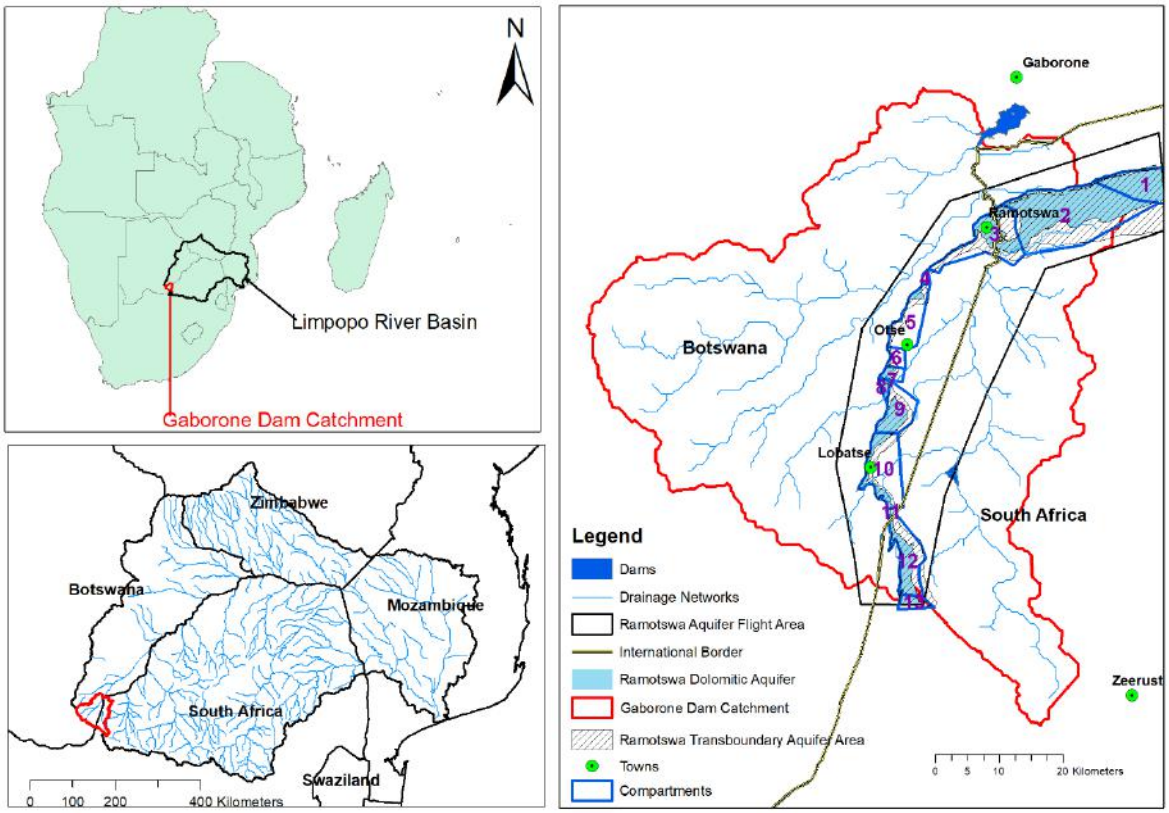

Figure 1: Study area location

2.2 Selected study area

The selected study area for the present study is shown in Figure 2. It covers compartment 3, and has an area of 80km^2. The Ngotwane River crossing the study area forms the international boundary. The annual precipitation ranges from 86-915 mm/a. The mean annual precipitation is 493 mm/a, standard deviation of ± 222mm [1995-2015]. There is high inter annual variability in annual rainfall (coefficient of variation of 45%). The long-term mean monthly rainfall data is shown in Figure 3. About 57% of the mean annual rainfall occur from January-March and 33% occur during October- December.

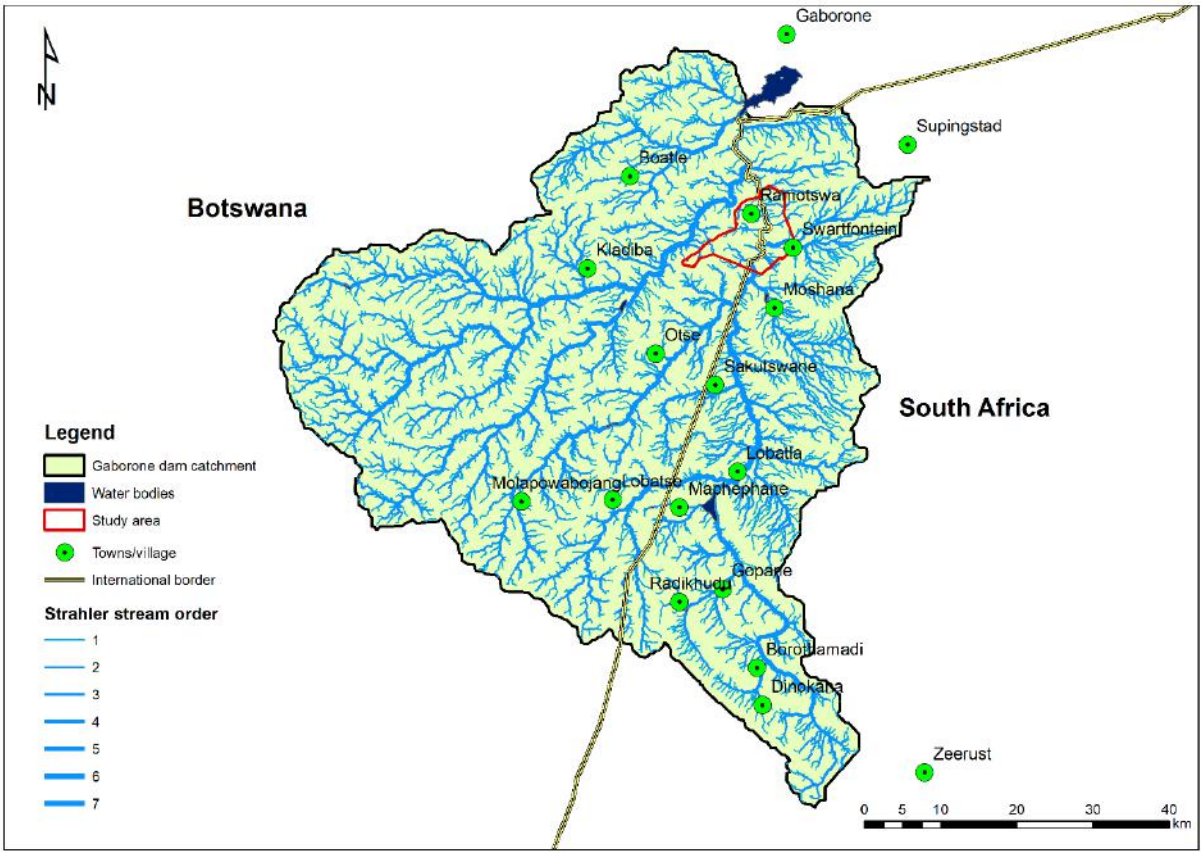

Figure 2: Selected study area location and Gaborone dam catchment stream order

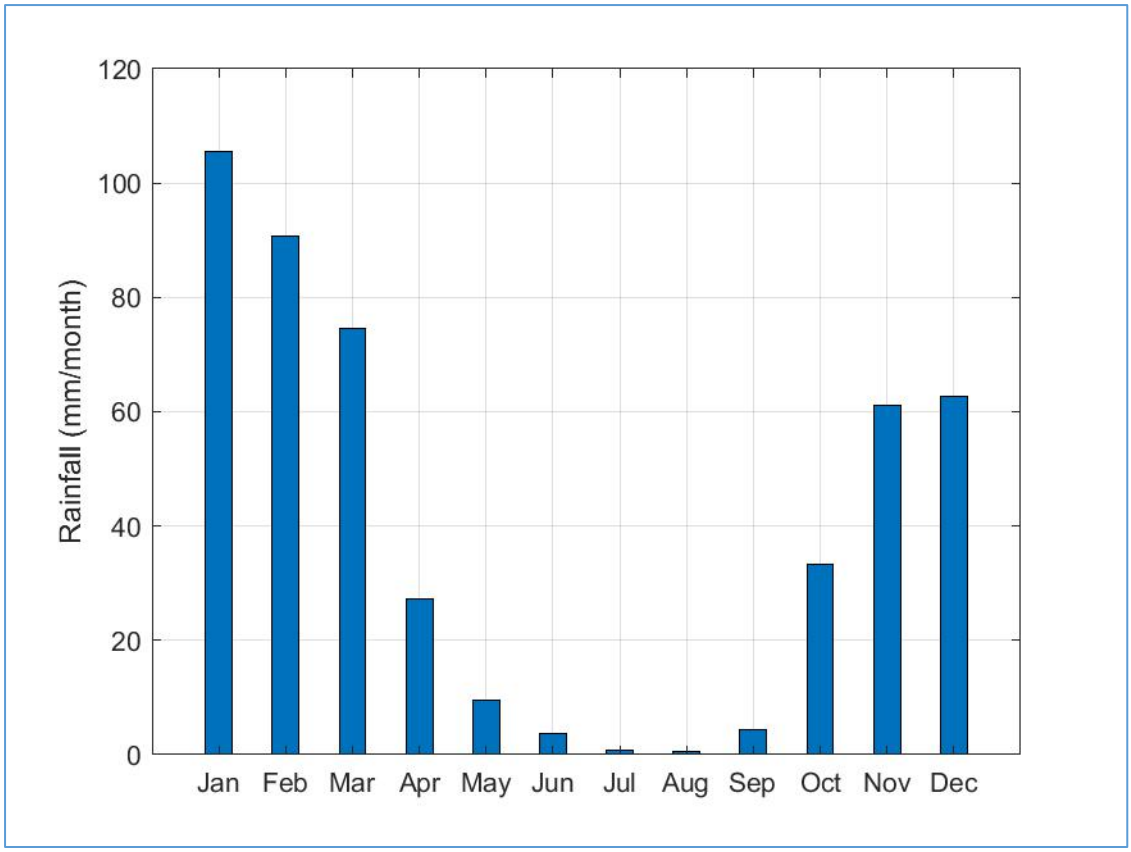

Figure 3: Mean monthly rainfall of Ramotswa station [1986-2014]

2.3 Land use and Land cover

Land use /land cover map was extracted from European Space Agency (ESA)[1]. The land cover map was produced from Sentinel-2A observations from December 2015-Decmeber 2016. The Sentinel based Africa land use and land cover map (20 m resolution) consists of 10 classes. Figure 4 shows the land use/land cover types in the study area and Table 1 presents the percentage area of each land use/land cover type. As shown, approximately 45% of the study area is covered by shrubs.

[1] http://2016africalandcover20m.esrin.esa.int/

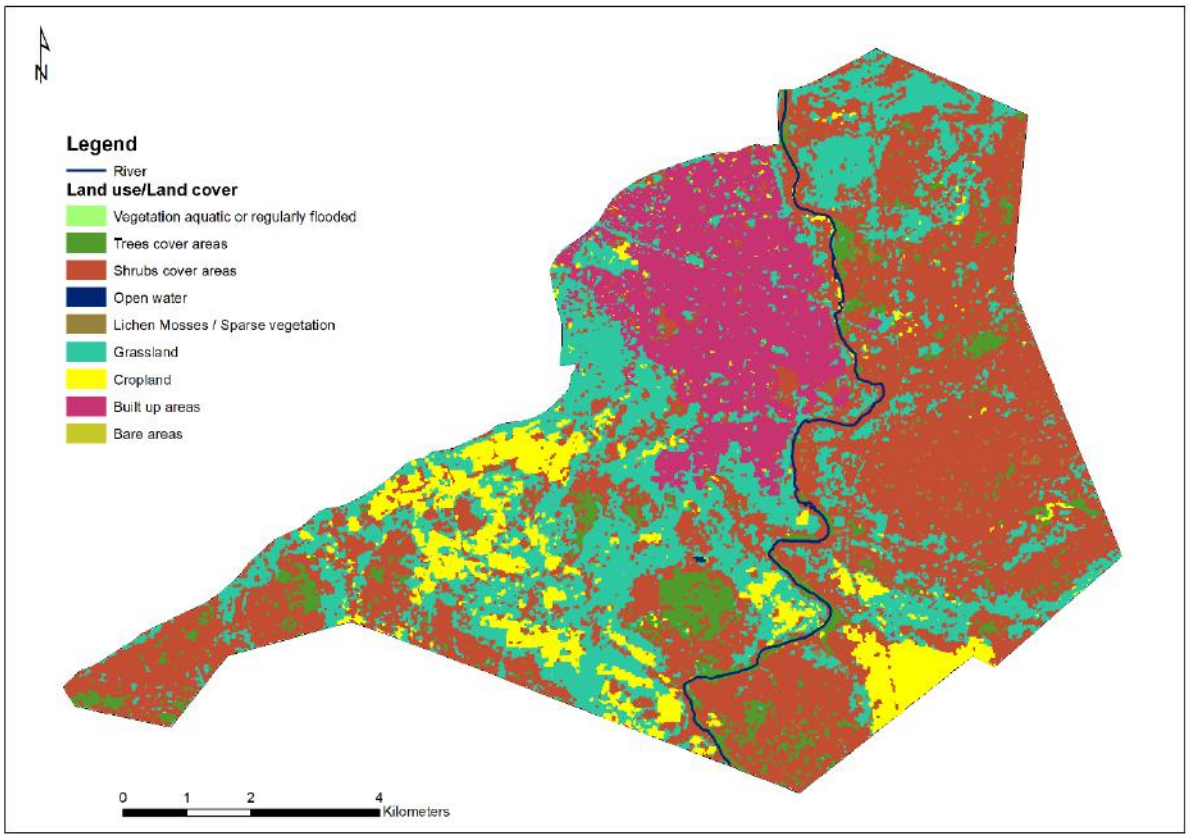

Figure 4: Land use/Land cover of Ramotswa

Table 1: Percentage of area covered by different land use/land cover types.

Land use/land cover type	Area (km^2)	% area covered by land use type
Shrubs cover areas	36.02	44.96
Grassland	22.28	27.81
Built up areas	10.26	12.80
Cropland	6.64	8.29
Trees cover areas	4.48	5.59
Lichen Mosses / Sparse vegetation	0.39	0.49
Bare areas	0.04	0.05
Open water	0.01	0.01
Vegetation aquatic or regularly flooded	0.00	0.00

2.4 Soil type and texture

Soil type for the study area was determined from the Soil Atlas of Africa (Figure 5). The percentage area covered by each soil type is presented in Table 2. As shown in Figure 5, Regosols, accounts about 68.0% of the area. Soil texture classes and spatial distribution were determined using the global soil dataset (SoilGrids, 250 m, https://soilgrids.org). The ISRIC-World Soil Information soil texture class classification utilizes United State Department of Agriculture (USDA) soil texture triangle and divided soils based on their relative amounts of clay, silt and sand into 12 soil types (Hengl et al., 2017). Soil

texture class map is available for 7 standard soil depths (0, 5, 15, 30, 60, 100 and 200 cm). The main soil texture class in the study area is sandy clay loam and covers about 97.6% of the area (Figure 6).

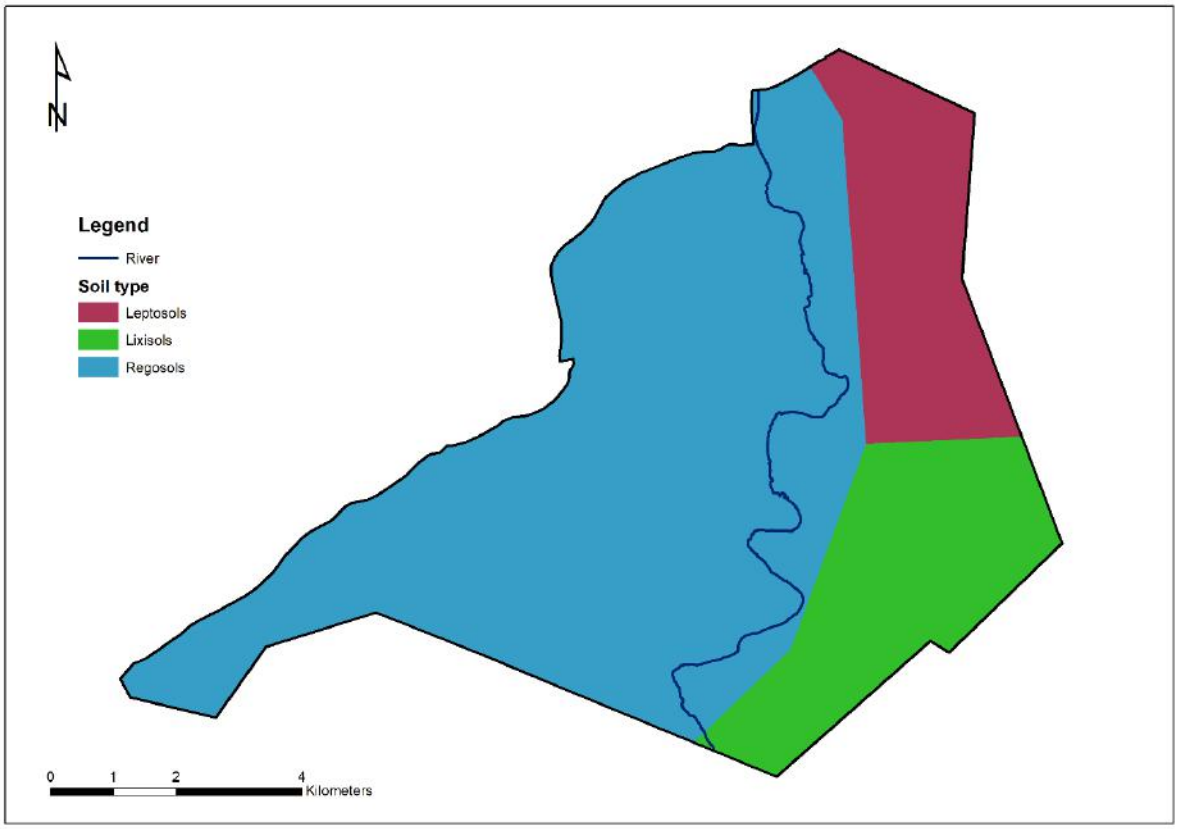

Figure 5: Soil type of the Ramotswa aquifer

Table 2: Percentage of area covered by different soil types and descriptions from Soil Atlas of Africa (Jones et al., 2013)

Soil reference group name	Percentage area (%)	Description	Detailed descriptions
Regosols	68.0	Weakly developed soils in unconsolidated material (from Greek *rhegos*, blanket)	Regosols are weakly developed mineral soils in unconsolidated medium and fine-textured material – more coarse-textured soils are Arenosols (in the case of sand) or Leptosols (in the case of gravel). Regosols show only slight signs of soil development - some accumulation of organic matter producing a somewhat darker topsoil is often the only evidence of soil formation. Limiting factors for soil development range from low temperatures, prolonged dryness, characteristics of the parent material or erosion. Regosols are extensive in eroding lands such as mountains or deserts where soil formation is generally absent.

Lixisols	17.3	Slightly acid soils with a clay-enriched subsoil and low nutrient-holding capacity (from Latin lixivia, washed-out substances)	Lixisols are slightly acid soils that show a distinct increase in clay content with depth. The clay is predominantly kaolinite with limited capacity to hold nutrients. Occurring mainly in the dry savannah region with low biomass production, Lixisols do not hold much organic matter and lack a well-developed soil structure. High-intensity rainfall will destroy any soil structure present making Lixisols prone to erosion. If the soil is not protected, a crust may develop which prevents rain entering the soil. Overland flow will then erode the topsoil, which is the most fertile part. Wind erosion may be an issue as loose soil particles at the surface can easily be blown away.
Leptosols	14.7	Shallow soil over hard rock or gravelly material (from Greek leptos, thin).	Leptosols are shallow soils over hard rock, very gravelly material or highly calcareous deposits. Because of limited pedogenic development, Leptosols have a weak soil structure. Leptosols occur all over Africa, especially in mountainous and desert regions where hard rock is exposed or comes close to the surface and the physical disintegration of rocks due to freeze/thaw or heating/cooling cycles are the main soil-forming processes.

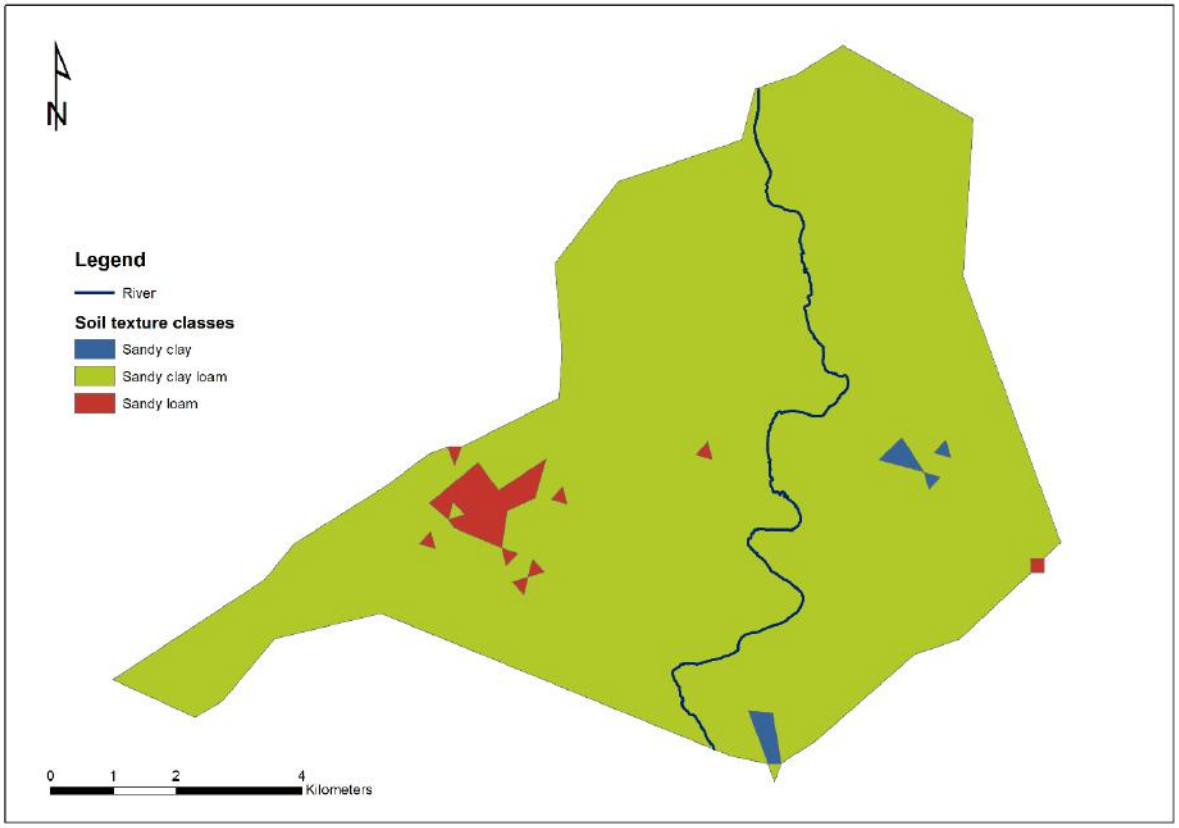

Figure 6: Soil texture calss of Ramotswa at depth of 200 cm from ISRIC (250 m resolution)

2.5 Geology

Geologically, the study area is formed from the Transvaal Supergroup. The Transvaal Supergroup from bottom to top consists of Black Reef Formation, the Chuniespoort group, and the Pretoria group. The Chuniespoort Group sitting on the top of the Black Reef formation further divided into the Malamani Subgroup consisting of the five dolomitic formation (from bottom to top: Oaktree, Monte Cristo, Lyttelton, Eccles and Frisco formation), Penge Formation and the Duitschland Formation. The division of the dolomite formation is based on their chert content. Unconformity of approximately 80 Ma exists between the Chuniespoort group and the upper Pretoria Group. The Perotia Group consists of the Rooihoogte Formation at the base. On top of the Rooighoogte formation is the Timeball Hill formation. Simplified geology of the study area is shown in Figure 7. For the Stratigraphy of the different formation readers are referred to Catuneanu and Eriksson (1999).

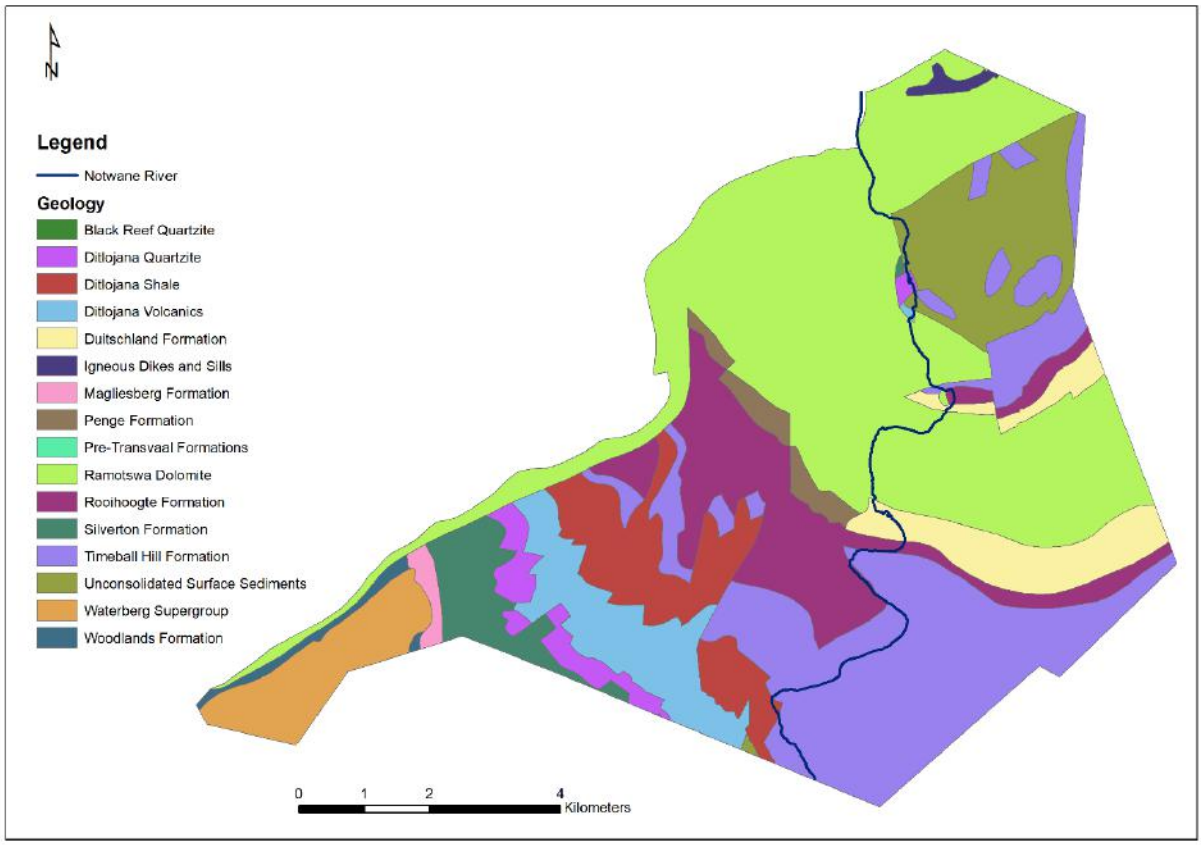

Figure 7: Simplified geology of the Ramotswa aquifer (Dolomitic formations are shown as one unit)

2.6 Hydrogeology

Two aquifer systems exist in the RTBAA, the most productive dolomite aquifer and the low yielding Lephala formation. The Ramotswa Dolomite comprises five carbonate formations referred to as either “chert-free” or “chert-rich” dolomite. While the chert rich formation Eccles and Mont Chisto are classified as a good aquifer, Oaktree, Lyttelton, and Frisco are regarded as poor aquifers. The Lephalae formation in Botswana is used to represent the formation sitting on top of the dolomite formation. Figure 8 shows interpolated groundwater level contour maps obtained by kriging. Although the general understood regional groundwater flow direction is from South to North following watershed/topography, at local level groundwater level contours slope towards the river.

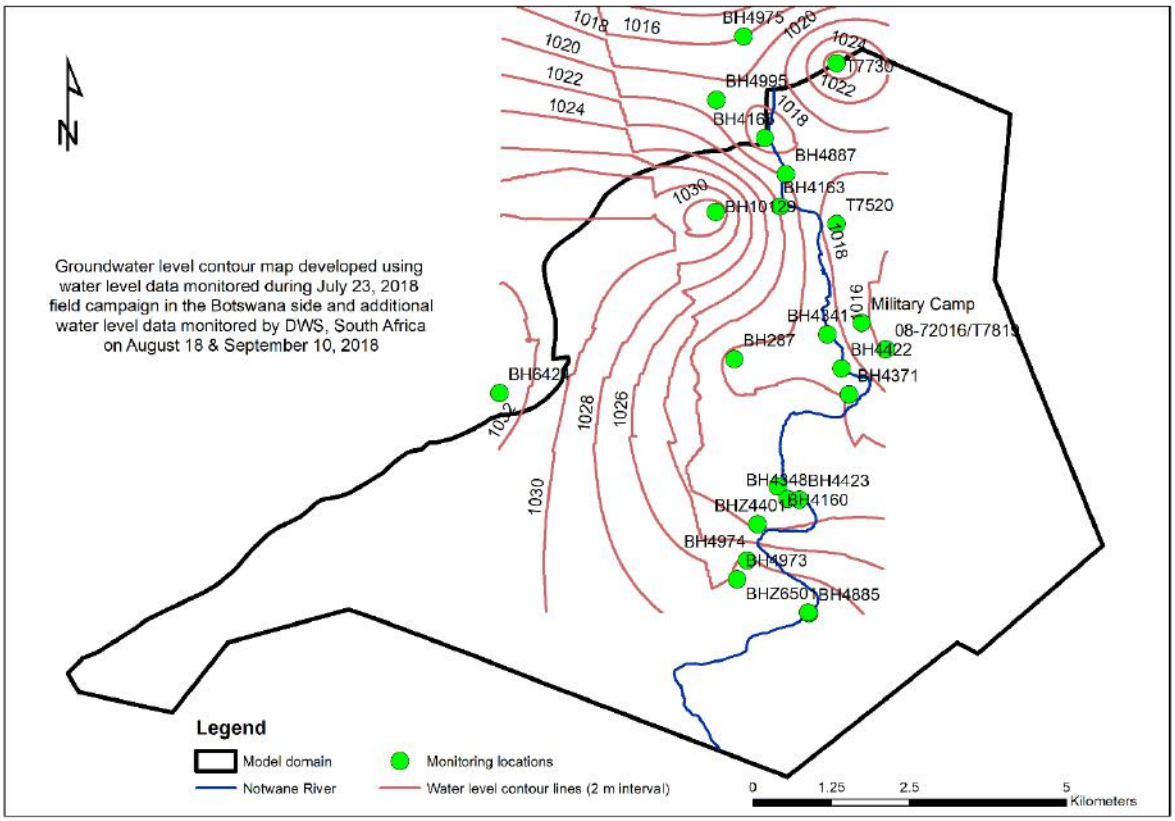

Figure 8: Groundwater level contours interpolated using kriging from groundwater levels monitored during field campaign July 23, 2018 and some additional water level data form South Africa side. In total 24 water level measurement were used for spatial interpolation

3. Review of geochemical reactions affecting water quality in karstic aquifer

The purpose of this section is to review the relevant geochemical reactions affecting water quality in karstic aquifer, particularly when the natural condition is modified during MAR application. Identified geochemical reaction of concerns will be used as a basis for risk assessment and geochemical modelling (See section 10).

3.1 Geochemical reactions of concern

Water quality improvement during MAR can be achieved through Soil Aquifer Treatment (SAT). SAT is a typical kind of surface spreading technique used for the purpose of water quality improvement. Treated wastewater is recharged using infiltration pond is treated while the infiltrated water passes through the soil and unsaturated zone. Water quality improvements in nutrient and pathogens is achieved through this process. If the SAT systems are designed in such a way that it provides adequate residence time, water quality improvement, e.g. inactivation of pathogens, degradation of organic chemicals and removal of N can be achieved (Vanderzalm et al., 2010).

However, changes in water quality can occur due to mixing between two dissimilar water types and interactions with the aquifer matrix (Vanderzalm et al., 2010). Long-term equilibria between groundwater and aquifer minerals are likely to be disturbed by MAR and the understanding of reactions of concern is essential for the feasibility of MAR (Herczeg et al., 2004; Vanderzalm et al.,

2010). One of the major concern of MAR application in karstic aquifer is dissolution of carbonate or dolomite (Herczeg et al., 2004; Vanderzalm et al., 2010). Dissolution can result in the development of conduits and sinkholes (dolines) which make the aquifer more vulnerable to contamination due to fast transport process (Daher et al., 2011). Clogging due to the precipitation of Fe and Mn hydroxides, due to a combination of microbial, hydrological and geochemical processes is another concern in the application of MAR in karstic aquifer, if not in all aquifer settings (Medina et al., 2013). Description of the main reaction of concerns in karstic aquifer are provided in the subsequent sections.

3.1.1 Dolomite dissolution

Carbonates are minerals which are dominated by carbonate ion CO_3^{2-}. The most common are calcite/calcium carbonate, $CaCO_3$, the main constituent of limestone and dolomite, calcium-magnesium carbonate ($CaMg(CO_3)_2$). Carbonate dissolution is a buffering process that can be induced by CO_2 present within the MAR source water itself (abiotic) or generated in situ by redox processes (biotic). The reactivity of the source water to carbonate minerals in the storage zone is influenced by the carbonate mineral saturation state and organic matter (Vanderzalm et al., 2010). The dissociation reaction of dolomite is presented in Equation 1. The solubility of dolomite at 25°C and a CO_2 partial pressure (P_{CO2}) of 10^{-3} bar is 50 mg/l, which can increase up to 300 mg/l (P_{CO2} = 10^{-1} bar). The range of abundance in waters is 10 – 300 mg/l. The solubility of calcite is 60 – 400 mg/l and gypsum is 2400 mg/l (Ford and Williams, 2013).

$$\boldsymbol{CaMg(CO_3)_2 + 2H_2O + 2CO_2 \leftrightarrow Ca^{2+} + Mg^{2+} + 4HCO_3^-} \quad (1)$$

The solubility of calcite and dolomite by dissociation in pure, deionized water is very low (14 mg /l), and rarely exceed the solubility of quartz (Ford and Williams, 2013). Most of the enhanced solubility of carbonite minerals is due to the hydration of atmospheric CO_2, which produces carbonic acid (Equation 2) which dissociates to provide H^+ (Equation 3), causing acid solution of calcite or dolomite. Other acids may provide additional H^+ and may further increase solubility.

$$\boldsymbol{CO_2(aq) + H_2O \Leftrightarrow H_2CO_3^0\ (carbonic\ acid)} \quad (2)$$

$$\boldsymbol{H_2CO_3 \Leftrightarrow H^+ + HCO_3^-} \quad (3)$$

The solubility of CO_2 is proportional to its partial pressure (Henry's law) and inverse proportional to temperature. P_{CO2} may increase in the soil as a consequence of organic compounds released in the rooting zone. The CO_2 productivity of roots or soil bacteria increases with temperature and water availability. The patterns of available soil CO_2 vary with soil type, texture and horizon depth, drainage and exposure, types of vegetation cover, soil flora and fauna as well as seasonal patterns in warming and wetting (Ford and Williams, 2013). For groundwater in carbonate aquifers, pCO_2 of $10^{-2.5}$ atm (Langmuir, 1997) – 10^{-2} atm, equivalent to a CO_2 content of 0.3 – 1 % of its volume, are considered normal (pCO_2 of open air $10^{-3.5}$ or 0.03 %). The pH of water in limestone and dolomite terrains usually falls between 6.5 – 8.9, where HCO_3^- is the predominant species and CO_3^{2-} being negligible below pH 8.3 (Ford and Williams, 2013).

The kinetics of dissolution of dolomite is an important factor. Calcite dissolves much quicker that dolomite, reaching equilibrium from sub-saturated fresh water in ten days or less while dolomite may require months or even years (White, 1988). For a P_{CO2} of $10^{-1.5}$ atm and a temperature of 10°C, achieving 95% dolomite dissolution would take 51 days while calcite dissolves in 10.7 hours (Parkhurst and Appelo, 2013). In addition to the composition of the aquifer and residence time of water (i.e. the

duration of water-rock interactions), water temperature has an influence on the dissolution of dolomite. Carbonates present exothermal dissolution heat, i.e. their solubility decreases as the temperature increases. This reduction is magnified by the fact that the solubility of CO_2 is also reduced as the temperature rises (Langmuir, 1997). On the other hand, the rate of dolomite dissolution accelerates with an increase in temperature (Herman and White, 1985; Moral et al., 2008).

3.1.2 Organic matter oxidation (through O2 or Fe(III) / SO42-)

The mixing of oxygenated surface waters with substantial amounts of dissolved organic carbon (DOC) or particulate organic matter with suboxic/anaerobic groundwater may result biochemical redox reactions that reduce the nutrient content via bacterial oxidation of organic matter (Equation 4) (Herczeg et al., 2004; Vanderzalm et al., 2010).

$$\boldsymbol{O_2 + CH_2O \Leftrightarrow CO_2 + H_2O} \quad (4)$$

As described above, the production of CO_2 further stimulate additional carbonate dissolution to buffer the acidity that is produced. When the dissolved oxygen is consumed, the main reactions are anaerobic organic matter oxidation via reduction of Fe(III) (Equation 5), and SO_4^{2-} (Equation 6) (Herczeg et al., 2004; Vanderzalm et al., 2010). This leads to an increase in the concentrations of mobile Fe, and H_2S.

$$\boldsymbol{FeOOH + CH_2O \Leftrightarrow Fe^{2+} + HCO_3^-} \quad (5)$$

$$\boldsymbol{SO_4^{2-} + 2CH_2O \Leftrightarrow H_2S + 2HCO_3^-} \quad (6)$$

3.1.3 Sulphide mineral oxidation (Pyrite)

Reduced minerals such as pyrite are likely to be oxidised when oxygenated surface water is introduced into an anoxic aquifer, competing with organic matter for reaction with injected oxygen. Arthur et al. (2005) reported this as one of the main water quality concern in MAR application due to the mobilisation of trace constituents such as As. According to Herczeg et al. (2004), acidity generated through sulphide mineral (Pyrite) oxidation may causes further carbonate dissolution (Equation 7). However, Herczeg et al. (2004), also highlighted that the impact of carbonate dissolution though Pyrite oxidation depends on the content of reactive pyrite in the storage zone and often considered to be limited unlike organic matter oxidation which expected to occur as long as source water with DOC is recharged.

$$\boldsymbol{\frac{15}{4}O_2 + FeS_2 \Leftrightarrow 2SO_4 + Fe(OH)_3 + 4H^+} \quad (7)$$

3.1.4 Ion exchange

Ion exchange usually occurs as a water-rock interaction process. Typical exchange reactions are between Ca^{2+} or Mg^{2+} with Na^+ or K^+ (Zhu, 2013). If Ca^{2+} is not sufficient to balance HCO_3^-, but the sum of Ca, Mg, Na are adequate, then this suggests ion exchange happened during injection, removing Ca^{2+} from solution for Na^+ and Mg^{2+} on exchange sites. The rate and extent of reactions is usually limited by the number of available surface sites, hence the effect of cation exchange on water quality declines with subsequent pore flushes, because with each flush, less exchange places will be available (Vanderzalm et al., 2010). According to Zhu (2013), Ion exchange is also an important reaction which accounts for significant changes in dissolved concentrations of trace metal cations. Unlike ion exchange, the influence of redox processes on injected O_2 and DOC removal is not expected to reduce

with subsequent pore flushes, but to be continued as long as nutrient source is available (Vanderzalm et al., 2010).

3.2 Clogging

Clogging is one of the main operational problem of MAR application which results in lower infiltration and recovery rates. Martin (2013) categorized the main factors that cause clogging into four. These includes:

1. *Chemical* due to precipitation of e.g. iron, manganese or calcite.
2. *Physical* e.g. by suspended solids in the injection water or clay swelling
3. *Mechanical*, such as entrained air/gas binding
4. *Biological*, which includes algae and (iron-) bacterial growth

In this section however, we mainly focus on chemical clogging as that is related to water quality. In most cases groundwater is anoxic and may have relatively high concentration of reduced species (e.g. reduced iron Fe2+). Therefore, infiltration of oxic water will lead to oxidation of some minerals e.g. precipitation of iron or manganese hydroxides (Medina et al., 2013). Iron incrustations are the most common and its removal is expensive and time-consuming (Houben, 2003). According to Medina et al. (2013) iron incrustations cause clogging of well screen , filter material, the pump itself and pipes transporting water to treatment plants. Significant iron incrustations occurs on the top part of the well, as this is the area where oxic water from the recharge water and anoxic water from the aquifer mix. Oxic water enters the well through the top of the well screen where it mixes with anoxic groundwater abstracted from deeper well sections, causing precipitation of iron hydroxides and promoting the formation of iron biofilms (Houben, 2003; Medina et al., 2013). Houben (2003) found high deposition rate of iron incrustations at the zone of high flow velocities (pump inlets/screen slots), probably due to higher oxygen contents of turbulent water. Degassing of CO_2 and an increase in pH further promotes the oxidation of Fe(II) (Houben 2003). According to Houben (2003), first scale precipitates of iron incrustations are mainly composed of poorly ordered ferrihydrite (high surface area) and over time it re-crystallises to the more stable phase Fe-oxides (goethite). This also results in a decrease in surface area, solubility, reactivity and an increase in thermodynamic stability and crystallite size. But, this process may take several years (Houben 2003). The half-time of abiotic oxidation of Fe(II) is quite variable due to its dependence on pH, O_2 and Fe(III) concentrations ranging from minutes to a couple of hours at neutral pH (Applin and Zhao, 1989).

The kinetics of Fe^{2+} oxidation (Equation 8) depend in the first order with respect to concentration of Fe^{2+} and partial pressure of dissolved oxygen P_{O2} and second order inversely proportional to pH (*k* is the reaction kinetics constant). According to Applin and Zhao (1989), iron incrustations cannot occur during pumping periods through abiotic oxidation of Fe(II) because reaction rate too low relative to residence time of water during pumping. Nevertheless, iron-incrustation is favoured by iron-oxidizing bacteria like *Gallionella* or *Lepthothirx* (Houben, 2003). According to Houben,(2003), wells provide a good environment for this bacteria as they are sedentary organisms (stay in the same location). Their presence has a catalytic effect on Fe(II) oxidation at lower pH values (range from 5.8 – 6.3) (Ralph and Stevenson, 1995). According to Ralph and Stevenson (1995) the growth of this bacteria is enhanced by the combination of low O_2 and high Fe(II) concentrations. They can profit during pumping from the presence of low O_2 that flows into the well in the upper well screen and high Fe(II) concentrations of

anoxic groundwater flowing upwards from the lower well screen section (Medina et al., 2013). Medina et al. (2013) found that frequent interruptions of well pumping could favour well clogging. These is because during the idle period of well operation, groundwater from the clogging zone leaks into deeper well/aquifer levels and may contribute to the dispersion of iron oxidizing bacteria, iron-hydroxides and bacterial slimes which may spread out and speed up the clogging process beyond the main clogging zone. Production boreholes in the Ramtowa is known to experience problem of iron encrustations (biofouling due to iron bacteria). This led to worn out of borehole casing and screens.

$$\boldsymbol{r = k(Fe^{2+})P_{0_2}(OH^-)^2} \quad (8)$$

Carbonate incrustations are associated with wells in carbonate-rich environments. Genesis depends on the degassing of CO_2 caused by turbulent flow inside the well, causing disruption of carbonate equilibrium and thus over-saturation and precipitation of carbonate minerals (Houben, 2003). On the other hand, Pavelic et al.(2007) reported that when nutrient rich recharge water is used, the process of further carbonate dissolution could intensify the enlargement of fractures and conduits, increasing groundwater storage and counteracting the impacts of aquifer clogging. Recharge water through MAR can become anoxic as it moves through sediments/soil due to organic matter degradation, depending on organic matter content and residence time (Medina et al., 2013). This could lower the oxidizing potential of the recharge water.

4. Water Source for MAR

Availability of recharge water of sufficient quantity and quality is the precondition for MAR application (Gale, 2005). Alternative source of water for MAR include surface water (perennial and ephemeral streams), urban storm water runoff, reclaimed wastewater, roof top rainwater harvesting, and groundwater transfer. Depending on the climatic, hydrologic, hydrogeological as well as an as anthropogenic activity in the area, MAR water from the various source could vary substantially both in quantity and quality. The intended use of the recovered water determine the required level of pre- and post-treatment. The main source of water for MAR is the the Ngotwane/Notwane ephemeral River flow. Other potential source include wastewater from the Ramotswa village. The advantage of considering wastewater as a source is its availability throughout the year irrespective of the rainy season. The downside is that it required extensive pre-post-treatment and it would be very costly.

4.1 River water

Ngotwane River is the main ephemeral river that drains the study area. Ngotwane River flows intermittently following large and intense precipitation events during the wet season and mostly dry in other periods (Figure 9). The Ngotwane River represents the international border between Botswana and South Africa. Gaborone dam is one of the large dam constructed on the Ngotwane River. The earth-fill dam drains a catchment area of ~4,318 km^2. According to Wikipedia source, the construction of the dam begin in 1963 and completed in 1964. Between 1983 and 1985 the dam level was raised by 7 m to increase capacity reaching a maximum height of 25 m. The dam has a storage capacity of 141.1 Million cubic meter and surface area of 15 km^2. Most of the dam reservoir area is less than 3 m deep. The water from the Gaborone dam is mainly used to support the city of Gaborone for domestic and industrial but also for the city of Lobatse and Ramotswa village (CSO, 2009). When dam capacity falls below 5%, the reservoir fails to release water (example, this occur during the period of December 2014 – March 2016). For this reason, there is a restriction in the amount of water supplied from the dam when the dam level is becoming low (McGill et al., 2018).

There is no gauging station in the Ngotwane River hence, quantitative estiamte using discharge frequency analysis was not possible. As shown in Fgiure 3 the period between November- March has good rainfall (above 50 mm/month) hence may provide good runoff that can used for MAR. However, there are concerns about diversion of the Ngotowane River flow for MAR that may reduce water now available for storage downstream in the Gaborone dam (Mosses, oral communcation)..

Figure 9: Ngotwane river bed during dry season (July 2018) in Ramotswa

4.2 Treated wastewater

Treated wastewater from the Ramotswa wastewater treatment plant (WWTP) is another potential source of water for MAR. The advantage of considering wastewater as a source is its availability throughout the year irrespective of the rainy season. The downside is that it required extensive pre-post-treatment and it would be very costly.

The Ramotswa WWTP located in the north of the village was constructed in 1981 (Figure 10). The WWTP was expanded in 2001 due to population growth. The WWTP spreads over an area of 23 hectares and has a capacity design of 3000 m^3/d. During the dry season, the pond system is working as an evaporation system and hence, no effluent produced during this period (Martin, 2017). In other time the discharge from the WWTP drain to Ngotwane River and/or infiltrates into the aquifer. We estimated the total wastewater production from the WWTP based on population data. The population of Ramtoswa village in 2011 was 28952 and the population growth rate is approximately 3.4% per year (CSO 2014). Assuming linear population growth the population in 2018 is estimated to be about 36587. Assuming per capita water consumption of 58 l/d based on data 1988-2008 (CSO, 2009, the total wasewater prodcution in 2018 is estimated to be 2122 m^3 /d. If we assume that 40% of the household is connected to sewage system, the total wastewater production is approximately 849 m^3/d. Martin (2017), estimated the daily inflow to the Ramotswa WWTP to be 1500 m^3/d, increasing during the wet season due to additional storm water runoff. Based on the assumption of 40% of the population connected to the sewage system, Martin (2017) estimated outflow from the WWTP to be around 600

m^3 /d. With daily production rate of 849 m^3/d annually about 0.3 $x10^6m^3$ of water would be available from the WWTP.

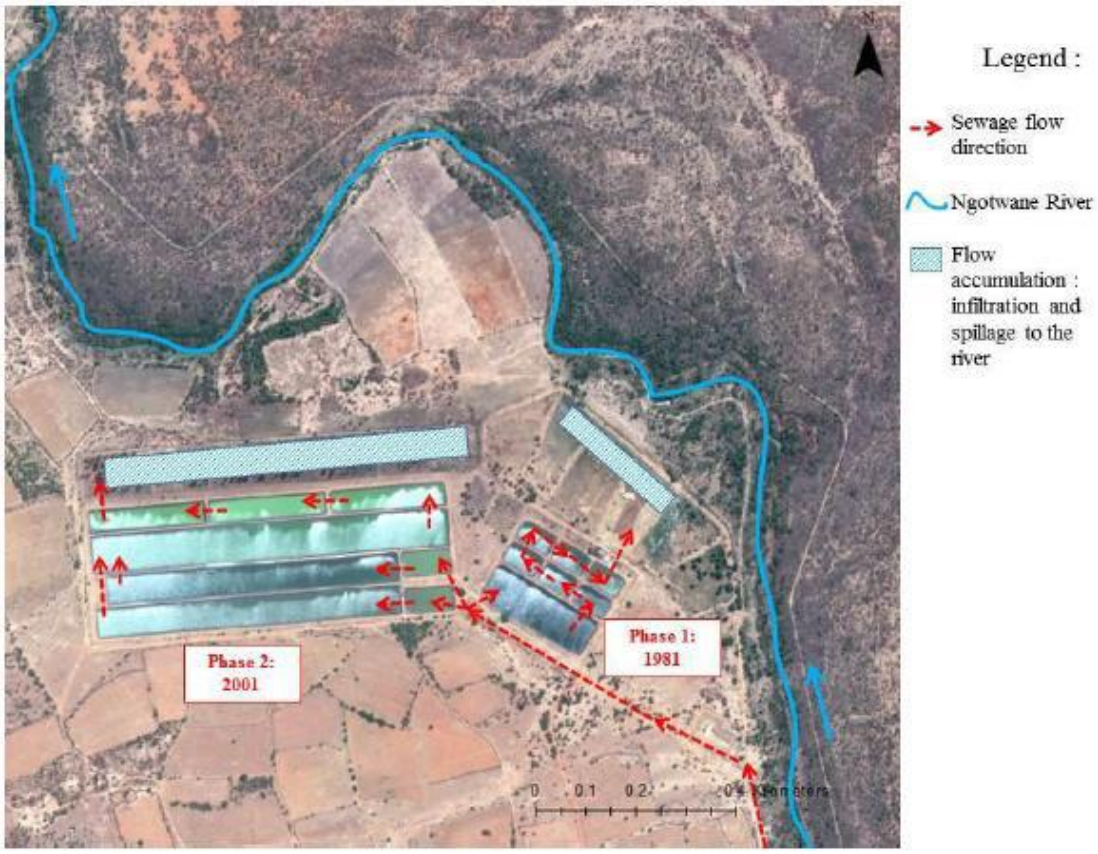

Figure 10: Sewage flow in Ramotswa WWTP (Martin, 2017)

5. Water quality characterization of source water and groundwater

The main objective of this section is to characterize water quality in the Ramotswa aquifer related to MAR water source and groundwater. To this end, River water quality for two station and groundwater water quality at seven selected observation wells were analysed. Figure 11 shows the location of River water quality monitoring sites and selected groundwater observation wells for water quality analysis. Water quality characterization results are presented in subsequent sections.

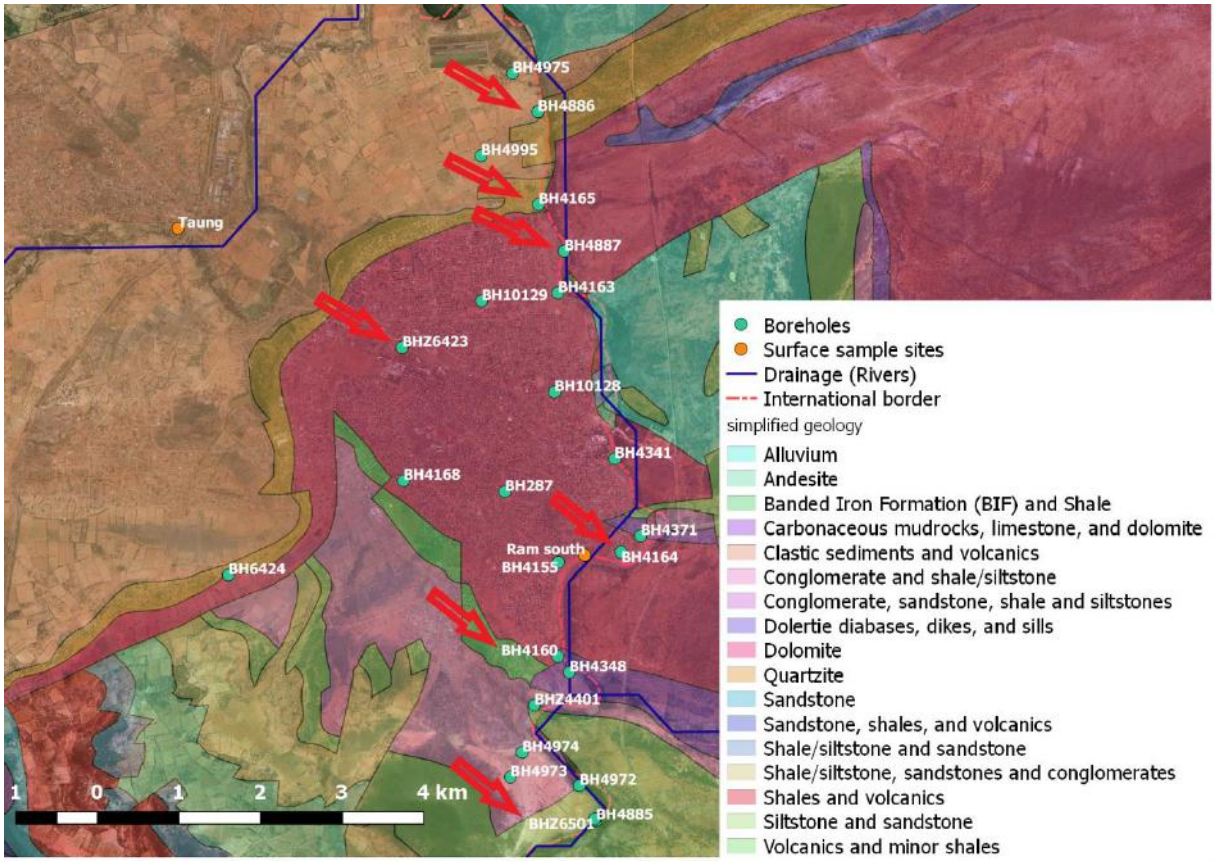

Figure 11: RAMOTSWA project area, boreholes, surface water sampling sites and simplified geology. Red arrows indicate the location of the selected boreholes.

5.1 Surface Water Quality

River water quality data was obtained from PULA project for the period of May 2017 – May 2018 for two sites (at Ngotwane River at the Ramotswa South and at Taung River, N-W direction from Ramotswa village) (Figure 11). The River water quality data do not have measurements of HCO_3^- and nitrate (NO_3^-), hence, charge-balance error accuracy check was not possible. Table 3 shows some descriptive statistics for the available river water samples from the two sampling sites. As can be seen in Table 3, River water samples form the Ngotwane River are dominated by Mg^{2+}compared to Taung River. Samples from Taung River have higher Na^+ and Cl^- concentrations compared to Ngotwane River suggesting more salinity. Figure 14 shows the electrical conductivity (EC) values at the two monitoring sites. High temporal variability in mineralization of River water samples is evident from Figure 12. Major ions concentrations at the Ngotwane River is presented in Figure 13. High concentration in Mg^{2+} is evident from this graph which is associated to dolomite. Although not measured high $HCO_3^-$is likely given the chemical characteristics of dolomite. The pH value in the area is in the range of 7.06 – 9.67 (data not shown).

Table 3: Descriptive statistics of available river water samples for two sampling sites: Ramotswa South (Ngotwane river) and Taung River(n=8). Data in mg/l

	Mean Ram	Min Ram	Max Ram	Mean Tau	Min Tau	Max Tau
Cl	23.67	1.43	43.88	37.13	1.52	78.04
SO_4	19.39	2.90	27.14	26.53	2.91	55.56
Ca	25.35	4.70	44.25	22.46	5.67	33.36

Mg	49.50	4.28	64.00	16.85	3.01	28.95
K	3.14	2.24	4.48	9.47	3.99	13.20
Na	16.87	3.26	28.20	32.12	2.36	61.50

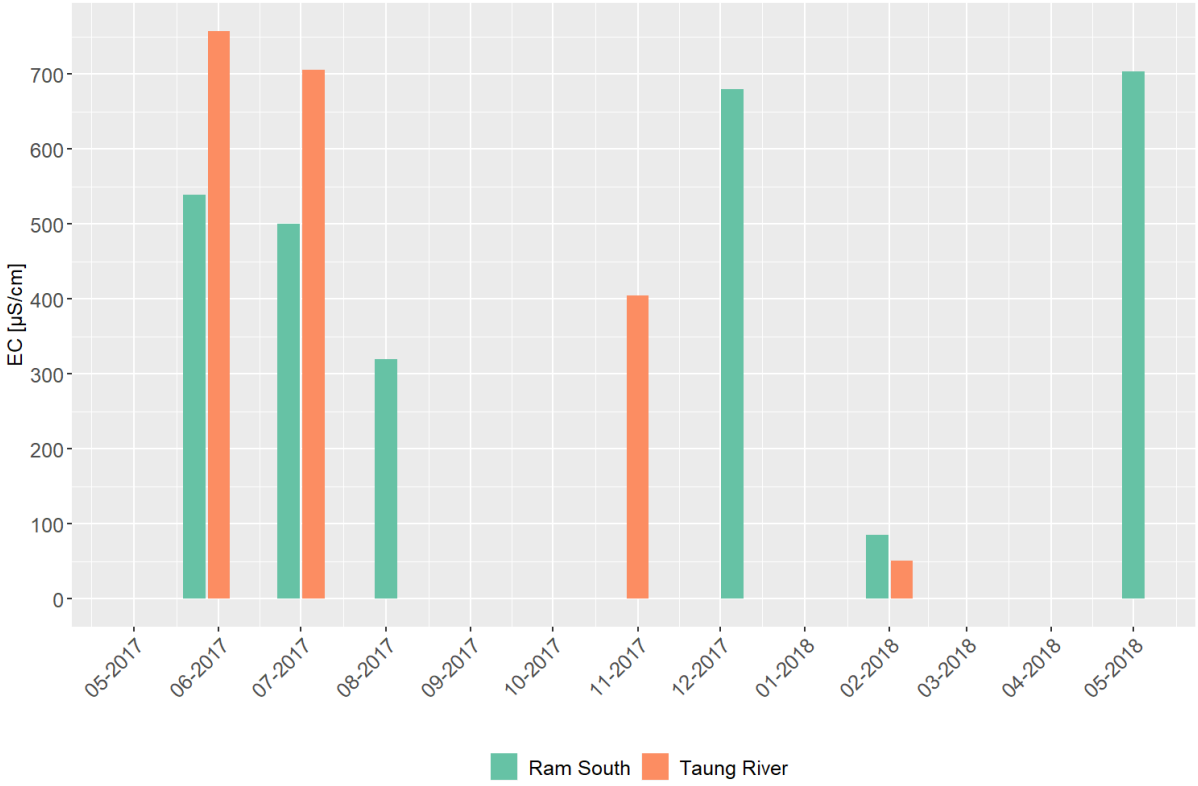

Figure 12: EC for two sampling sites on the Ngotwane Rive (Ram South) and Taung River

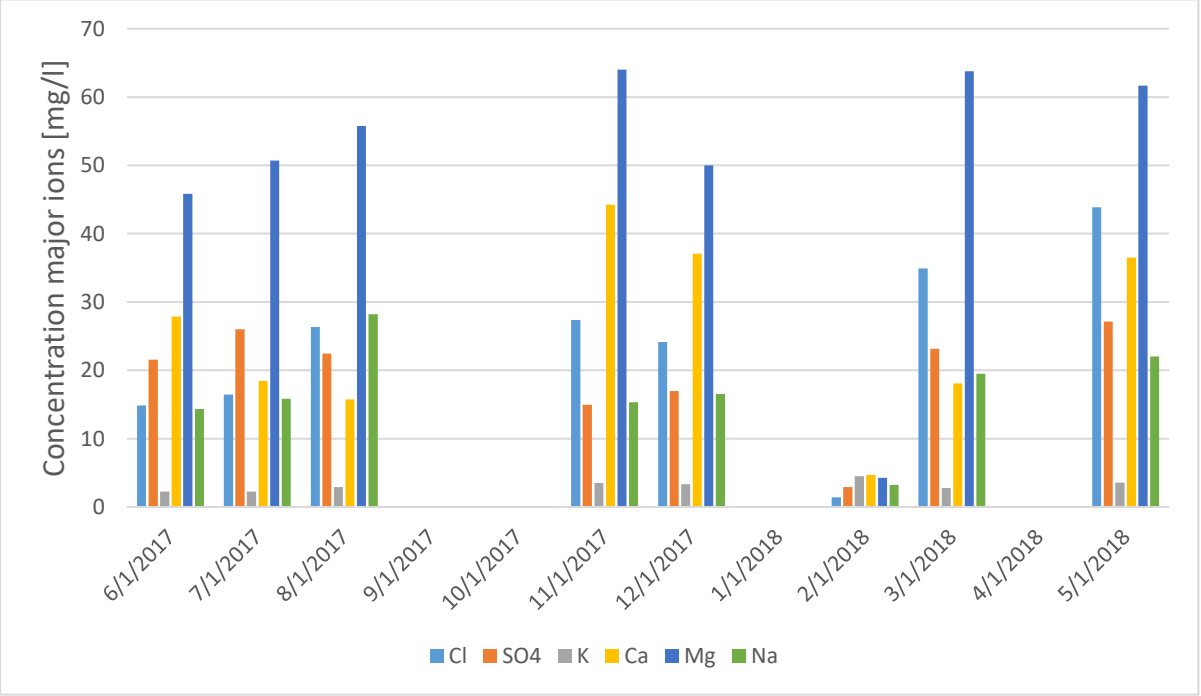

Figure 13: Ngotwane river water quality data (major ions) samples on location "Ram south"

5.2 Groundwater Quality

Since groundwater quality data in most observation boreholes are incomplete, representative groundwater quality monitoring boreholes were chosen based on their proximity to river channel, spatial location (South, Centre, and North) of the Ramotswa village. Table 4 provides a summary of selected observation boreholes for water quality analysis, geology, relative location and approximate distance to Ngotwane River. The selected boreholes have relatively consistent water quality data for the period 2001-2012.

Table 4: Summary of selected groundwater quality observation wells

Observation well	Geology	Location	Approximate distance to the river (m)
BH6501	siltstone/sandstone	South	5
BH4160	dolomite/carbonaceous mudrocks and limestone	South	200
BH4164	dolomite	Centre	500
BH6423	dolomite	Centre	Very far
BH4887	dolomite	North	10
BH4886	clastic sediments and volcanics	North	500
BH4165	quartzite (close to dolomite)	North	100

5.3 pH, EC, TDS

The mean value of PH, EC and TDS of selected observation wells is presented in Figure 14. The mean PH values ranges from 7.22 (Bh6501) - 8.23 (BH4886). The mean EC across the selected observation well ranges from 585.11 µS/cm (BH6423) – 1117.89 µS/cm (BH4886). Similarly, the mean TDS value ranges from 344.78 mg /l (BH6423) – 671.78 mg /l (BH4886). High value in EC could be due to rock dissolution or enrichment of Na^+, Cl^- or NO_3 while lower EC values could indicate probably a better connection to the conduit and fracture network, with higher flow velocities and lower water-rock interactions (Xanke, 2017) or a dissolution of groundwater with low mineralized surface water. Ford and Williams (2013) stated that TDS > 450 mg/l in waters in carbonate areas is an indicator for chloride, nitrate or sodium enrichment. This value is exceed in all the 5 selected observation boreholes except BH6423 and BH4887.

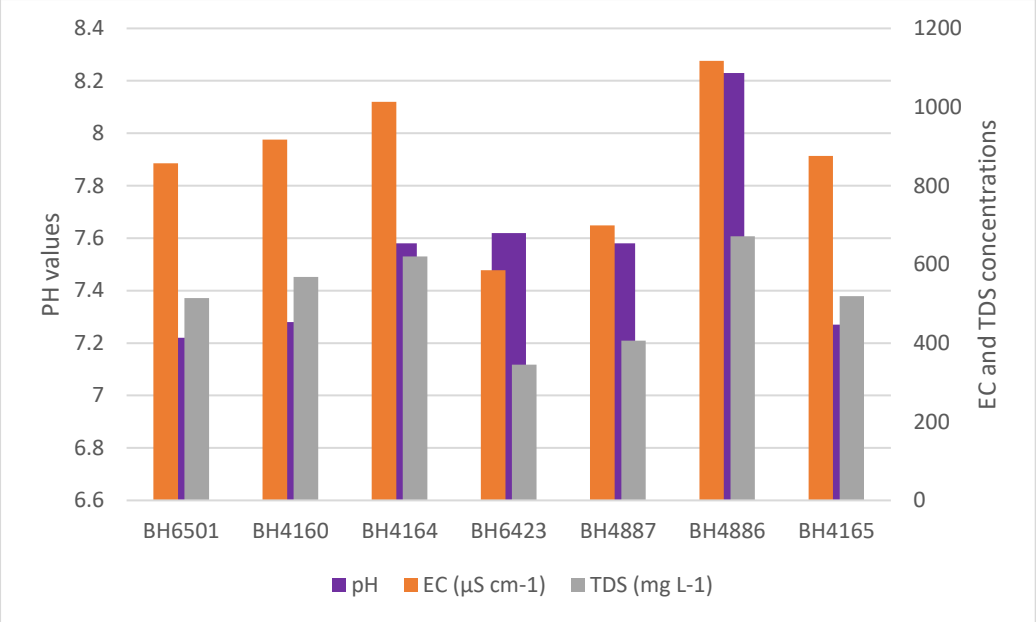

Figure 14: Mean PH, EC and TDS values at selected boreholes

5.3.1 Major ions

According to Sundaram et al. (2009), few major ionic species constitutes about 95% of the ions in most groundwater, this include the positively charged cations sodium (Na^+), potassium (K^+), calcium (Ca^{2+}) and magnesium (Mg^{2+}), and the negatively charged anions chloride (Cl^-), sulphate ($SO4^{2-}$), bicarbonate (HCO^{3-}) and nitrate ($NO3^-$). Figure 15 shows the concentration of these major ions in the selected observation wells in the Ramotswa aquifer. It is important to notice that the spatial variability of r Ca^{2+}, NO_3^-, Na^+, Cl^- and SO_4^{2-} is high in the area.

A graphical representation of the chemistry of groundwater quality data of the seven selected observation boreholes shown in piper diagram (Figure 16). As shown in Figure 16 most of the samples are dominated by $Ca^{2+}$and Mg^{2+}, indicating that the dissolution of dolomite is the dominant process controlling groundwater chemistry in the study area. Only the samples from BH4165 and BH4886 in the north of the study area are of Na(K)-HCO_3 type or Na(K)$ClSO_4$ type, suggesting that probably anthropogenic influence affecting groundwater quality. The order of the abundance of the major ions in all groundwater samples is $Mg^{2+} > Ca^{2+} > Na^+ > K^+ = HCO_3^- > Cl^- > SO_4^{2-}$. The possible reasons for the spatial variability is discussed in the section 5.2.3.

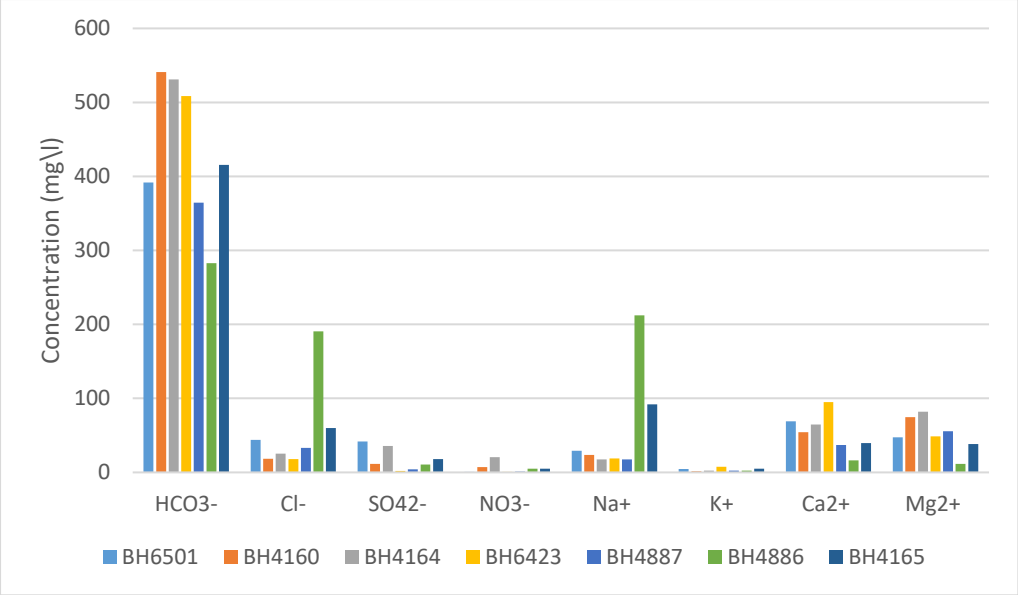

Figure 15: Mean concentration of major ions in seven selected observation boreholes

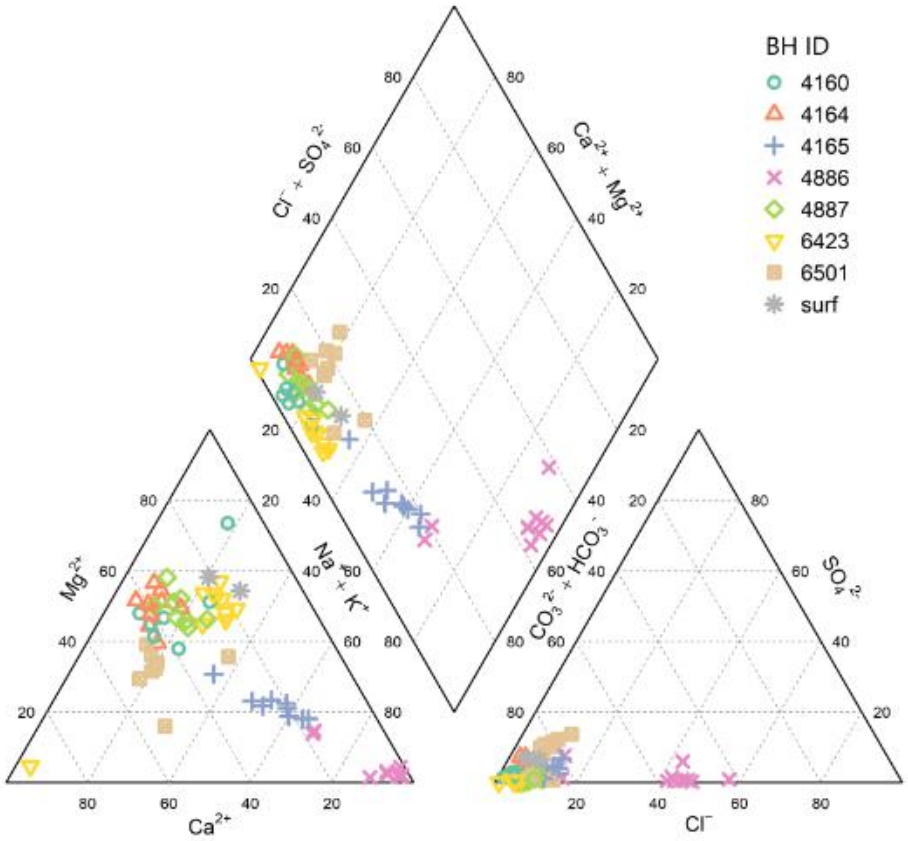

Figure 16: Piper diagram displaying water samples from selected boreholes of the Ramotswa study area and two river water samples ("surf") from the Ngotwane river. Most samples are dominated by magnesium, calcium and bicarbonate, hence high proportions of sodium and chloride are present in borehole 4886 north of Ramotswa.

5.3.2 Spatial viability in major ions

Calcium and Magnesium The mean Ca^{2+} concentration across the selected observation well ranges from 16.07 mg/l (BH4886) – 95.04 mg/l (B4623). The mean Mg^{2+}concentration ranges from 11.44

mg/l (Bh4886) – 81.91mg/l (BH4164). Maximum concentrations in $Ca^{2+}$and Mg^{2+} occur in observation wells located in the dolomite aquifer while the minimum occur in the observation well located in the Ventersdorp Supergroup (consisting of clastic sediments and volcanics). Dolomite dissolution could be the reason for high concentration, but, surprisingly, BH6501 in the Lephale formation (Rooihoogte formation) shows high Ca^{2+} concentration (69.05 mg/l), suggesting that other geochemical process play some role. BH4623 which is very far away from the river showing high concentration also contradict that the assumption that distance to the river is controlling the degree of karstification (dolomite dissolution). BH4887 is located north of Ramotswa close to the river (~10m), yet low in Ca^{2+} (37.02 mg/l) and Mg^{2+} (55.51 mg/l) concentrations. The slow dissolution of dolomite or dilution with low mineralized surface water could be an explanation for low Ca^{2+} and Mg^{2+} concentrations. Valdes et al. (2007) noted that the dominant major ions such as HCO_3^-, Ca^{2+} and Mg^{2+} are autochthonous (originating where found), and they may occur due rock dissolution controlled by pH and CO_2 partial pressure. The maximum allowable limit for Mg^{2+} in drinking water according to the Botswana drinking water standard is 100 mg/l (BOS, 2000). High Mg^{2+} concentrations could result in risk of cardiovascular disease (WHO, 2009).

Bicarbonate The mean HCO_3^- concentration across the selected observation well ranges from 282.59 mg/l (BH4886) – 540.98 mg/l (BH4160). High concentration of HCO_3^-may be attribute to dolomite dissolution (Jiang et al., 2009). BH4160 is located in the dolomite formation while BH4886 is in the Ventersdorp Supergroup (consisting of clastic sediments and volcanics). At BH 4886, low concentrations of HCO_3^- may be due to high pH which results low acidity.

Sodium, The mean Na^+ concentration ranges from 17.49 mg/l (BH4164) - 212.02 mg/l (BH4886). The ions Cl^-, Na^+, SO_4^{2-} and NO_3^- are known to be principally have an allochthonous origin (originating in a place other than where found), and hence, they may be originated from atmospheric inputs, human activities in the catchment or agriculture (Valdes et al., 2007). Natural sources of high Na^+ concentrations are the dissolution of halite or albite. The dominant geology at BH 4886 are Siltstones (Greywackes) and Quartzites. Greywackes contain quartz and feldspar. One popular member of feldspar group is albite ($NaAlSi_3O_8$). The high pH (8.1) may suggest that process of dissolving alkaline salts (Na_2CO_3) in the soil level are intensive (SOLOVEY and JÓŹWIAK, 2008). However, it is more likely that the origin in the study area is due to anthropogenic influence, which can be chemical fertilizers ($NaNO_3$) or domestic effluents as observed in other study areas (Edmunds et al., 2003; Jiang et al., 2009; Valdes et al., 2007). Cation exchange between Ca^{2+}, Mg^{2+} and Na^+ is also possible, but according to Edmunds et al. (2003) it is less relevant in Chalk aquifers. There are no health-based guidelines for sodium, but it may affect taste >200 mg/l (WHO, 2003c).

Chloride The mean Cl^- concentration ranges from 17.76 mg/l (BH6423) – 190.66 mg/l (BH4886). High concentrations in Cl^- are correlated to high Na^+ concentrations. High Cl^- concentrations are often associated with pollution sources such as industrial and domestic effluents, fertilizers (KCl) and leakages of septic tanks (Edmunds et al., 2003; Jiang et al., 2009; Valdes et al., 2007; Xu et al., 2017). BH4886 is outside of the populated area of Ramotswa village but, close to both fields (fertilizer) and Ramotswa wastewater treatment plant which may have influence on groundwater quality. Chloride concentrations over 250 mg/l may affect taste of the water, although there are no health-based guidelines (WHO, 2003a).

Sulphate The mean SO_4^{2-} concentration ranges from 1.76 mg/l (BH6423) – 41.58 mg/l (BH6501). Geogenic sources of SO_4^{2-} can be the dissolution of gypsum or anhydrite ($CaSO_4$), which are not known to be present in the study area. The most likely reason for SO_4^{2-} source is the oxidation of pyrite (FeS_2). The geology at BH6501 is characterized through black, graphitic and pyritic shales (Lephala formation). Pyrite oxidation will increase sulphate concentrations and acidity, resulting in higher dolomite dissolution. The oxidation is intensified if more oxygen enters subsurface, for instance through MAR. Anthropogenic sources of sulphate can be wastewater (Xanke, 2017) or fertilizer ($(NH_4)_2SO_4$) as well as effluents from septic tanks and livestock waste in the residential areas (Jiang et al., 2009). There is no health-based guideline for sulphate in drinking water (WHO, 2004).

Iron and manganese concentration were only tested during sampling in the years 2001, 2003 and 2004. Iron concentrations at different boreholes exceeded the maximum allowable concentration of 2000 µg/l (BOS, 2000) by far, with a maximum measured concentration of over 9000 µg/l at BH6423. The most common sources of iron and manganese in groundwater are natural through the weathering of iron and manganese bearing minerals and rocks. In the study area, there are several iron-bearing formations: the Penge formation, a banded iron formation, the Magopane formation (chert, highly ferruginous at top) and the Lephala formation (contains among others pyritic shales). However, not all boreholes with high iron concentrations in groundwater are near those formations (e.g. BH6423 is in the dolomite, BH4165 in the Black Reef Quartzite). Industrial effluent, acid-mine drainage, sewage and landfill leachate could also contribute iron and manganese to local groundwater. Anaerobic groundwater may contain Fe(II) at concentrations of up to 10 mg/l without discoloration or turbidity in the water when pumped directly from a well. Turbidity or colour may develop in piped systems at iron levels above 0.05-0.1 mg/l. Iron also promotes undesirable bacterial growth ("iron bacteria") within a waterworks/distribution system, resulting in the deposition of a slimy coating of the piping. High iron concentrations in drinking water will become noticeable in taste. The WHO does not propose a health-based guideline for iron(WHO, 2003b)

A critical concern in operational aspects of MAR can be aquifer or well clogging caused by precipitation of Fe or Mn hydroxides, resulting in lower infiltration or recovery rates. The infiltration of oxic surface water in an anaerobic groundwater through MAR can change redox conditions and favour precipitation reactions of dissolved Fe^{2+} (or Mn^{2+}, Mn^{3+}, Mn^{4+}). The formation of iron (or manganese) encrustations is caused by a combination of microbiological, geochemical and hydrological processes (Medina et al., 2013).

Four samples exceeded the maximum allowable limit of 500 µg/l for manganese (BOS, 2000). Mn concentrations > 0.1 mg/l impart an undesirable taste to (WHO, 2011a). Oxidation of Mn(II) compounds result in encrustation problems. Contents > 0.05 mg /l can cause discoloration. Anaerobic groundwater often contains elevated levels of dissolved manganese. Mn^{2+} dominates in most waters at pH 4-7 but more highly oxidized forms may occur at higher pH values. The WHO guideline for manganese in drinking water is 400 µg/l, also, contrary to inhalation, oral consumption of manganese is regarded less dangerous for humans. However, consumption of water with very high concentrations of Mn can cause neurological diseases (WHO, 2011a).

Nitrate The mean NO_3^- concentration ranges from 0.66 mg/l (BH6501) – 20.72 mg/l (BH4164). Recent study also identified elevated NO_3^- concentration in most boreholes in Ramotswa (McGill et al., 2018). The high nitrate concentrations in the Ramotswa aquifer has led to the shutdown of the Ramotswa

wellfield in 1996, because groundwater exceeded the national drinking water standard for nitrate and the lack of capacity to treat the water (McGill et al., 2018; Ranganai et al., 2001). It was reopened in 2014 as an emergency source of water because of low dam levels in Gaborone. High nitrate concentrations can reduce the ability of the red blood cells to carry oxygen to the vital tissues, especially for infants of six months or younger. The resulting illness is called methemoglobinemia or "blue baby syndrome"(WHO, 2011b).

Generally, there is no known lithologic source of nitrate. Increased concentrations are referred to agricultural and sewage effluents (Jiang et al., 2009). This assumption is strengthened by the fact that almost all boreholes with high NO_3^- concentrations are situated inside the village. McGill et al. (2018) found out that human waste leaching from pit latrines and septic tanks are likely to be the source of nitrate contamination. The use of pit latrines increases particularly in times of water scarcity, as it was the case during the recent drought from 2013-2016 (McGill et al., 2018). Particularly vulnerable are sites where groundwater levels are shallow, because natural retardation processes are not effective in removing nitrate from the polluted water and pollutants can enter the aquifer directly through the distinct karst system (McGill et al., 2018; Ranganai et al., 2001). Groundwater levels in the study area are shallow, and it is possible that groundwater is in direct contact with pit latrines, favouring nitrate leaching into groundwater. A natural process for *in situ* bioremediation of NO_3^- pollution is denitrification in low oxygen conditions, denitrifying microbes reduce NO_3^- into N_2O and N_2. Naturally, the occurring concentrations of DOC in groundwater limit denitrification.

5.4 Reclaimed wastewater

Wastewater quality data is not available. However, Martin (2017) measured inflow and outflow from the WWTP twice in 2017 and found high concentrations in suspended solids, oil and grease and ammonia in inflow. According to Martin (2017), industries such as Bolux Milling, Higro feeds (both food industry) and Ramotswa Glass Works could be the main sources. High contents in oil and grease could cause physical blockages of sewers, pumps and screens. Furthermore, oxygen transfer rate is reduced which diminishes the efficiency rate of the degradation of suspended solids and biological oxygen demand (BOD) in facultative ponds. Nitrogen is still present as ammonia in discharge, which can be oxidized in nitrate and nitrite and could contaminate the river and the aquifer (Martin, 2017). Due to the fact that samples were collected during the wet season, water quality is expected to be worse during dry season (Martin, 2017).

In addition since most of the population use on-site sanitation unmanaged grey water and wastewater infiltration into the aquifer may result aquifer contamination. Since no maintenance exists, leakage of sewage pipes constitutes an additional challenge, posing threat of direct leakage of raw wastewater into the aquifer (Martin, 2017). One of the main problem of the Ramotswa WWTP is that, the WWTP function as evaporation pond and this could not be efficient for industrial wastewater and unless pre-treatment by the industries is carried out. During the dry period there is not outflow from WWTP. Due to poor wastewater quality, MAR using treated wastewater would require a high level of pre-treatment to be of sufficient quality.

6. MAR Method

Due to the high degree of heterogeneity, MAR in karst aquifer is very challenging. Karst processes at the surface and underground affect the infiltration process (Daher et al., 2011). The presence of conduits that quickly drain the recharged water without significant storage and its vulnerability to

contamination makes MAR in karst aquifer challenging (Daher et al., 2011). Understanding how karst features control ground-water flow and respond to varying hydrologic conditions is critical for effective planning and implementation of MAR (Green et al., 2006), because groundwater management options appropriate for other aquifer may not be adequate for karst aquifers. Hence, MAR must be approached in an appropriate and rational manner to ensure the success of MAR in karst aquifers (Daher et al., 2011).

Recharge to karst aquifers should be operated in such a way that concentrated flow through sinkholes and conduits are avoided, otherwise, the filtering capability of the soil will be compromised, recharged water will be lost through discharge areas. Daher et al. (2011) recommended to target the epikarst zone for potential MAR application mainly for two reasons: (i) spreading the injected water preferably through slow and diffuse infiltration, and (ii) favouring natural treatment process. An epikrast is a term used to refer the highly weathered carbonate rock below the soil layer and typically 3-10m deep but in some cases it may extends to 30 m or more (Ghasemizadeh et al., 2012; Williams, 2008). The high porosity and permeability of the epikarst is due to its proximate to the main source of carbon dioxide in the soil that results dissolution of carbonate (Williams, 2008). Epikrast zone play significant role in recharge regulation that allow slow and delayed infiltration and it has the potential of distributing the recharge water into different infiltration process (Daher et al., 2011) such as: fast infiltration though large openings, slow infiltration through fine cracks and rock porosities. Under natural conditions some of the recharge may pass through the concentrated flow paths such as sink holes. MAR operation in Karst aquifers must be operated in such a way that water flow though concentrated fast infiltration flow paths are avoided (Daher et al., 2011). It is strongly recommended that water be injected far from karst features such as vertical shafts or closed depressions, which are generally connected to the conduit system, so as to ensure that the recharge water spreads towards the phreatic zone through diffuse and slow flow conditions (Daher et al., 2011).

The present study assumes that the preferred method of MAR in the Ramotswa Transboundary Aquifer is the spreadign method, for at least four reasons. First, the spreadign method is low cost and practically simple to apply. Second, spreading methods are a preferred method for MAR in karstic aquifer as they allow spreading of recharge water through slow and diffuse infiltration(Daher et al., 2011). Third, the spreading method allows a natural treatment process. Fourth, spreading method/ infiltration basins offer the opportunity for clogging control.

7. Soil infiltration Test

7.1 Determining soil infiltration using double ring infitrometer

Soil infitration rate is the rate water enter the soil. Infitration process is the most complex hydological process that contorls, among others, the rainfall-runoff and surface water-gorundwater proecesses Burke, 2009; Gray and Norum, 1967). The infiltration rate decreases as the soil becomes saturated. If the precipitation rate exceeds the infiltration rate, runoff commences. Factors affecting soil infitration rate inlcudes: soil texture, land use, antecedent moisture content,soil densisty (Haghnazari et al., 2015; Gray and Norum, 1967).

In the field, soil infitartion is measured using an infiltrometer. There are two types of infiltrometer viz., flooding type and rain simulators. In this study soil infitration rate is measured using double ring

infiltrometer method. Double ring infiltrometer was developed to overcome some of the limitations in single ring infiltrometer such as estimating the over infiltration rates as water in the single ring is not purely vertical but it also diverges laterally. To eliminate the effect of surrounding dry soil on the infiltrometer, the double ring uses two concentric rings because the water in the outer ring forces vertical infiltration of water inside the inner ring, thereby reducing lateral movement of water in the soil from the inner ring. The double ring infiltromter consists of a 30 cm and 45 cm diameter rings as shown in the Figure 17. The main objective of infiltration test is twofold: 1) determing riverbed infiltration rate and iniftration rate outside of the river bed and constrain model parameter related to focused recharge estimation and improve model concpetualization. 2) Determining soil infitration rates at selected site so that it can be used for MAR assessment through scnearion analysis using Hydrogeolgoical model. Figure 18 shows infitation test sites in the river bed and outside of the riverbed in the Ramotswa Aquifer. Figure 19 shows iniftration test site photo where there is an existing practice in water harvesting. The double-ring infiltrometer is applicable only in soils where an adequate seal with the rings can be established

Two techniques can be used with the double-ring infiltrometer, one is constant-head method and the other is falling-head method. For the constant-head method, water is systematically added to both the inner and outer rings and the volume of water required to maintain a constant water level of inner-ring at constant time intervals was measured and used to calculate the infiltration rate. The infiltration rate is the amount of water per surface area and time unit which enters the soils. The depth of water in ring was measured by a hook gage and metal measuring tape, while a stop watch was used to measure time.

Figure 17. Double ring infitrometer apparatus

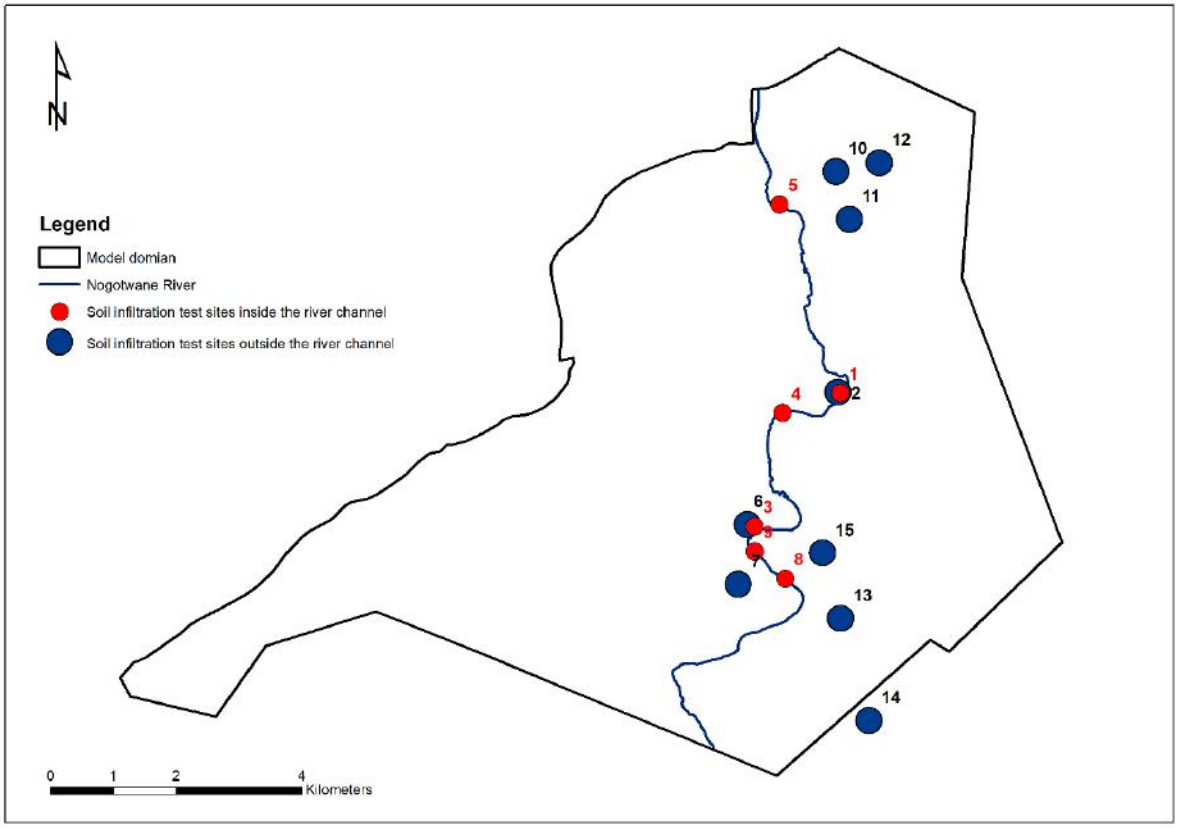

Figure 18: Soil infitration test sites in the Ramotswa aquifer (Labels in the dot corssponds to site ID in Table 5)

Figure 19. One of the several ponds used for holding water for livestock watering when it rains. These ponds are known by community to increase recharge into the groundwater (infiltration site ID 11)

7.2 Procedure

1. The infiltrometer ring is driven carefully on a flat surface into the soil with a hammer to a depth of about 10 cm or until it firmly fixed to avoid water leakage between the thin wall of a ring and soil. A flat metal frame placed on top of the rings was used for driving rings uniformly into the soil.
2. After fixing the rings in the soil, the test area was immediately pre-soaked for 1 hour using 30-minute intervals prior to testing, by filling outer and inner rings to a known mark with water.
3. The fall in water level from the inner ring for the first 30 minutes was measured from the change in floater levels.
4. The rings were then refilled and change in water level from the inner ring measured for the second 30 minutes.
5. The minimum water depth in the rings before refilling should be 10.2 cm, if the infiltration is fast and the rings are drained faster than the 30-minute time interval. The drop in the water level during the second 30 minutes of the pre-soaking period was used to determine the time interval between readings during the test (Burke, 2009). When the water level drop was 5.1 cm or more, 10-minute measurement intervals were used and where water level drop was less than 5.1cm, 30-minute measurement intervals were used.
6. The readings of water level drop in the centre ring at either 10 or 30 minutes were recorded. After each reading, both rings were refilled to water level indicator mark.
7. Measurements of drop in water level continued at the selected interval determined during the pre-soaking period until a minimum of eight readings were taken or until a stabilized rate of drop was obtained, whichever occurred first. The termination of test occurred after a maximum of two hours of measurement plus the 1-hour pre-soaking time.
8. A stabilized rate of water drop from inner ring was one in which a difference of 0.64 cm or less of drop was observed between the highest and lowest readings of four consecutive readings (Burke, 2009). This drop that occurs in the centre ring during the final period or the average stabilized rate, expressed as cm per hour, represented the point infiltration rate for that test site.

7.3 Soil infiltration test results

Table 5 shows the summary of the infiltration tests in the Ramotswa area. Sites 1-9 are in Botswana, while sites 10-15 are in South Africa. Site in South Africa show high infiltration rates from open bush areas to old fields. Site 11, inside a dry pond showed the lowest infiltration (0.403 m/d) due to fine sediments deposits in South Africa. This result is consistent with riverbed channel from sites 3, 4, 5, 8 and 9 in Botswana. Rate of infiltration decreases with time and become constant – basic infiltration rate (infiltration capacity). Typical infiltration graphs from the four sites are shown in Figures 21.

The infiltration rate is generally lower inside the river channel compared to areas outside the river channel. The average infiltration for areas outside the river channel (2.568 m/d) was higher than infiltration inside the river channel (0.504 m/d) in Botswana side of Ramotswa. However, field observation of some sections of the river channel showed weathered rock outcrops and infiltration is likely to be high for these sections. Old and abandoned field recorded the highest infiltration and indicating suitability for infiltration ponds for MAR implementation.

Table 5: Summary of infiltration tests

Site	Testing date	Latitude (⁰)	Longitude (⁰)	Elevation (m)	Infiltration (cm/min)	Infiltration (m/d)	Comment

1	09/05/2018	-24.8845	25.88762	1022.0	0.0002	0.002	Inside river channel, near BH4337
2	09/05/2018	-24.88441	25.88731	1026.0	0.3115	4.486	Outside river channel, near BH4337
3	10/05/2018	-24.90355	25.87392	1026.0	0.0175	0.252	Inside river channel, near BH Z4401
4	10/05/2018	-24.8873	25.87852	1021.0	0.1450	2.088	Inside river channel, close to BH 4155
5	11/05/2018	-24.85734	25.87831	1015.0	0.0167	0.240	Inside river channel, near BH 4163
6	11/05/2018	-24.90326	25.87283	1025.0	0.1887	2.717	In the field with grass, near BH4401
7	11/05/2018	-24.91186	25.87132	1031.0	0.2025	2.916	In the field with grass, far upstream near mountain; southern boundary of compartment 3
8	27/07/2018	-24.91108	25.87871	1029.0	0.0125	0.180	Inside river channel, upstream catchment
9	27/07/2018	-24.90715	25.87395	1029.4	0.0187	0.269	Inside river channel, upstream catchment
10	23/10/2018	-24.85268	25.88725	1024.0	0.0640	0.922	Bare soil in thorny bushes
11	24/10/2018	-24.85954	25.88932	1032.0	0.0280	0.403	Inside a dry pond, on sandy sediments
12	24/10/2018	-24.85149	25.89406	1034.0	0.0940	1.354	Bare soil in thorny bushes (silt sandy)
13	24/10/2018	-24.91688	25.88739	1034.0	0.3350	4.824	Patches of dry grass in thorny bushes (sandy silt). Infiltration was fast
14	25/10/2018	-24.93156	25.89174	1051.0	0.4475	6.444	Old field with patches of dry grass (light coloured silty soil)
15	25/10/2018	-24.90746	25.88464	1035.0	0.4625	6.660	Old field with patches of dry grass (reddish silty soil). Infiltration was fastest of all sites

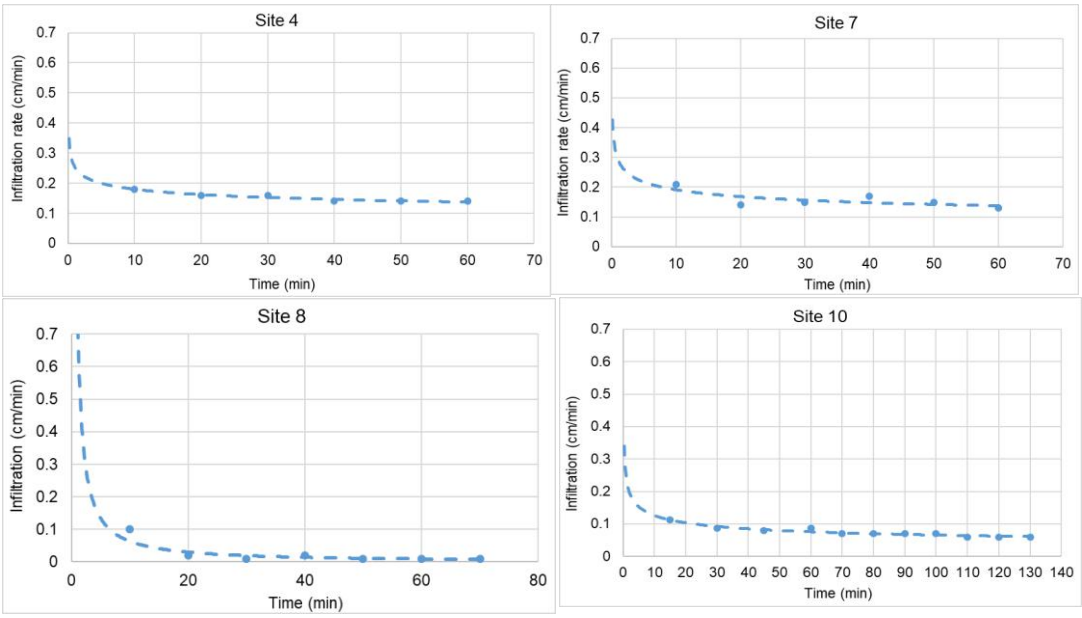

Figure 21: Selected four sample infiltration curves

9. Potential MAR site selection

The main aim of this section is to select potential MAR sites for spreading method based on multiple criteria. Ebrahim et al. (2017) developed MAR suitability map for the Ramotswa area based on four criteria: slope, lithology, soil and land use/land cover. These criteria were selected based on a comprehensive literature review (López, 2017). In this section we include some additional criteria (e.g. groundwater quality, depth to groundwater) and select potential MAR site for Scenario analysis using Hydrogeological model. These additional criteria were not included as part of the multi-criteria mapping because of lack of spatial data, rather, they were used to support potential site identification. Table 6 presents the favourable conditions for application of MAR using the spreading method.

Table 6: Site suitability for managed surface infiltration (Smith and Pollock, 2010)

Favourable condtions	**Unfavourable condtions**
Unconfiend aquifer with sufficiently thick vadose zone	Aquifers in which the basin bottom cannot be excavated into permeable strata
Vadose zone with large permeability and absence of flow-restricting layers	Existence of layers with small permeablity within the vadose zone
Adequate areal extent of permeable soils	Small aquifer transmissivity leading to excessive water table mounding
Sufficient aquifer transmissivity to prevnet excessive water table mounding, e.g., deep, wide conductive layers	Contamiants in the source water or vadose zone
Source water that is chemically compatiable with the receving groundwater	Shortage or inhibitive expense of land area
Source water and vadose zone that are free of contaminats	

9.1 MAR suitability map

MAR suitability assessment was carried out by applying a Multi-Criteria Analysis using Geographic Information System (GIS). The objective of the MAR suitability mapping was to enable initial assessment MAR in Africa. Based on literature review and availability of data, four criteria including: lithology, soil, slope and land use and land cover were selected and used for the suitability mapping. Because of its simplicity and less subjectivity the ranking method was used to assign criteria weights .The ranking method involves ranking of criteria according to their rank order or importance from the most important to the least. Then the weights are calculated by $((N-r+1)/\sum(N-r+1))$, where N is total number of criteria, and r is rank order. The suitability map produced based on this approach is presented in Figure 22. For more detail readers are referred to previous MAR suitability report by Ebrahim et al. (2017). Description of the four criteria used in the suitability mapping and additional

include to further refine the potential MAR site selection for MAR assessment using Hydrogeological model scenario analysis is presented in Table 7.

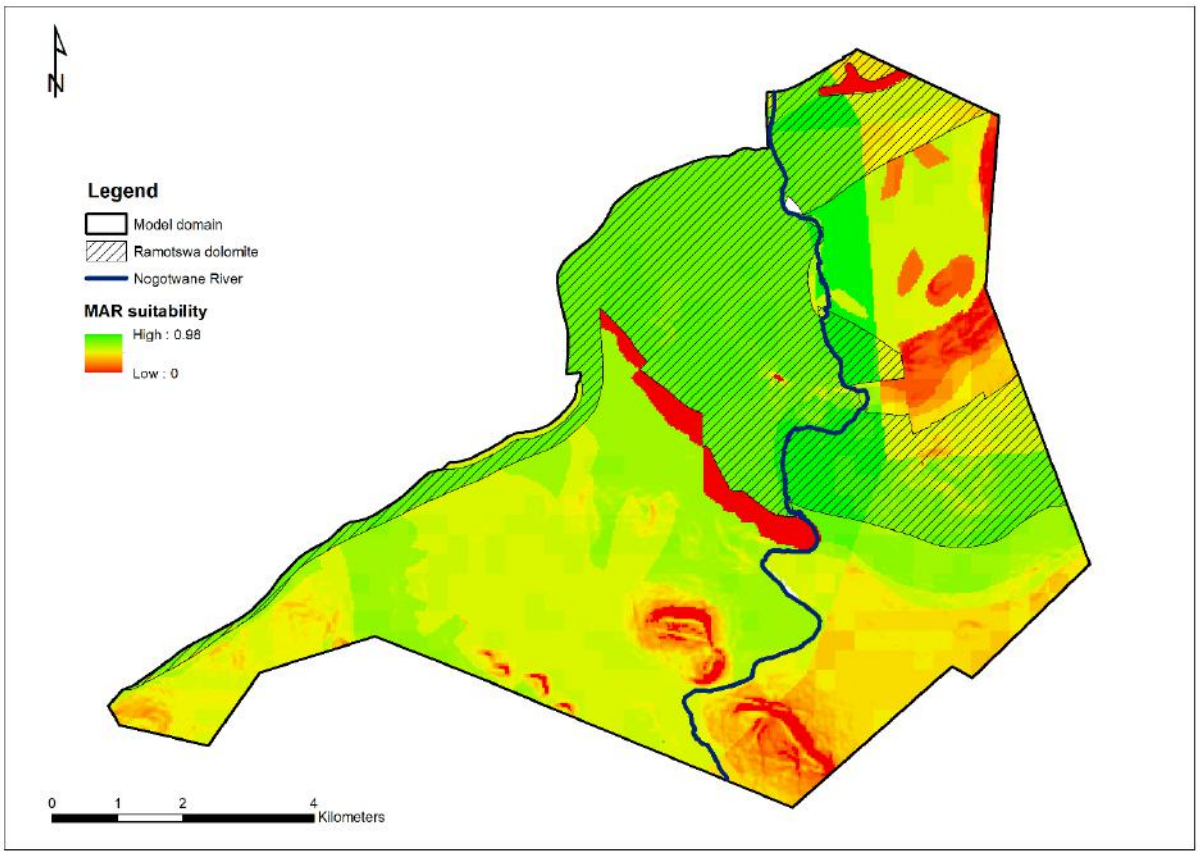

Figure 22: MAR suitability map for the Ramotswa Aquifer

Table 7: List of criteria chosen for MAR suitability assessment and their relevance for site selection

Criteria	Description
Slope (topography)	Runoff is directly related to slope angle. Flat areas allow higher infiltration rates and are more suitable for surface infiltration.
Soil texture	Soil properties significantly affect infiltration rates, which will decrease in general with increasing clay content of the soil. Low permeable soils are unsuitable for surface infiltration. Soil infiltration test conducted as part of this study were used to guide further selection of potential MAR sites. High soil infiltration rates are favoured.
Land use/cover	Land use/cover assessment in this study is based on the context of land clearing and land preparation requirement for MAR. Thus, highly vegetated areas are less preferred. Urbanized areas are non-feasible for MAR.
Lithology	Lithology determines aquifer permeability and storage, two main factors affecting MAR feasibility. Highly permeable aquifers can accept higher rates of recharge to store large volume of water. Low transmissivity can inhibit lateral flow away from the recharge area and result in groundwater mounds that interfere with the infiltration process. Very high transmissivities constitute the risk of lateral movement to discharge points

Groundwater levels	Depth to groundwater during the wet season is used to determine if sufficient storage for MAR is available. Furthermore, water quality improvements by natural attenuation processes increase with unsaturated zone thickness.
Groundwater quality (nitrate & iron)	Should be adequate at the place of recharge. High nitrate concentrations pose a threat to human health if recovered water is used for domestic purposes. High iron concentrations can cause clogging issues depending on the redox potential of aquifer and recharge water.
Distance to source (river)	Distance to the recharge source mainly affects infrastructure costs.
Distance to demand	Distance to the location where recovered water is used also affects infrastructure costs

9.2 Potential MAR sites

Based on suitability mapping six potential MAR sites, were selected and assessed using additional criteria such as depth to groundwater, water quality, and distance to source water. Soil infiltration test conducted during this study was also used to refine the MAR site selection. The six selected MAR potential sites is shown in Figure 23. Four sites were selected from the Botswana side (BT1, BT2, BT3 and BT4) and three from the South African side (SA1, SA2 and SA3). Figure 24 shows the minimum depth to groundwater for all observation wells in Ramotswa. Description of additional criteria assessment for each sites is given below. Figure 25 shows the final selected sites overlain with the MAR suitability map based on the four criteria.

BT1 The minimum depth to groundwater in this site ranges from 1.65 at BH4165 – 7.74 m (BH4995). From the depth to groundwater point of view the site has reasonable storage in the area around BH4995. However, the site has high nitrate concentration, mean of 136 mg/l at BH4995. In addition high sodium and chloride concentrations were measured at BH4886. High iron concentration is another challenge in this area. Mean iron concertation ranges from 867 µg/l (BH4995) - 4749 µg/l (BH4165). High iron concentration may results clogging problem.

BT2 The minimum depth to groundwater in this area ranges from 2.0 m (Bh4973) - 4.4 m (BH4973). The shallow depth to groundwater allow little opportunity for additional storage. However, the observed water level hydrograph shows that the depth to groundwater could reach 10 m during average rainfall years. The water quality in this area in general regarded as good. The nitrate level is low (0.26- 5.96 mg/l). But, the iron concentration is relatively high (383-5522 µg/l). Soil infiltration test conducted as part of this study show high infiltration rate.

BT3 The minimum depth to groundwater in this area is relatively deep, approximately 20 m at BH6424. Groundwater quality in terms of nitrate is very good (4.81 mg /l), but exceptional high iron concentrations have been measured at the borehole (mean 14433 µg /l). The distance from the river (recharge water source) is far approximately 3.2 km, which lead to relatedly high infrastructure cost compared to other sites.

BT4. The depth to groundwater in this site is also relatively deep. The minimum depth to groundwater is about 14.5 m (BH4168) and can provide sufficient groundwater storage. Nitrate concentrations at BH4168 are relatively high (mean 103.69 mg /l). The other challenge is that this site is located in the

urbanized Ramotswa village and land availability for MAR may be a challenge. It is also relatively far from the river (~2 km).

SA (SA1, SA2, and SA3) No groundwater level data is available in all sites in South African side. Hence, minimum depth to groundwater in each site is unknown. No water quality data is also available. Soil infiltration test conducted as part of this study at SA1 and SA3 shows that SA1 sites has moderate infiltration rate, while SA3 has very high infiltration rate. The water quality in SA1 and SA2 is expected to be good in terms of nitrate levels, but SA3 may have high nitrate as the area is farm land. Fertilizer application may cause elevated nitrate concentration. SA2 is also located in unconsolidated surface sediment formation which may provide good MAR storage potential. SA3 is close to drainage lines which is good for water harvesting for MAR.

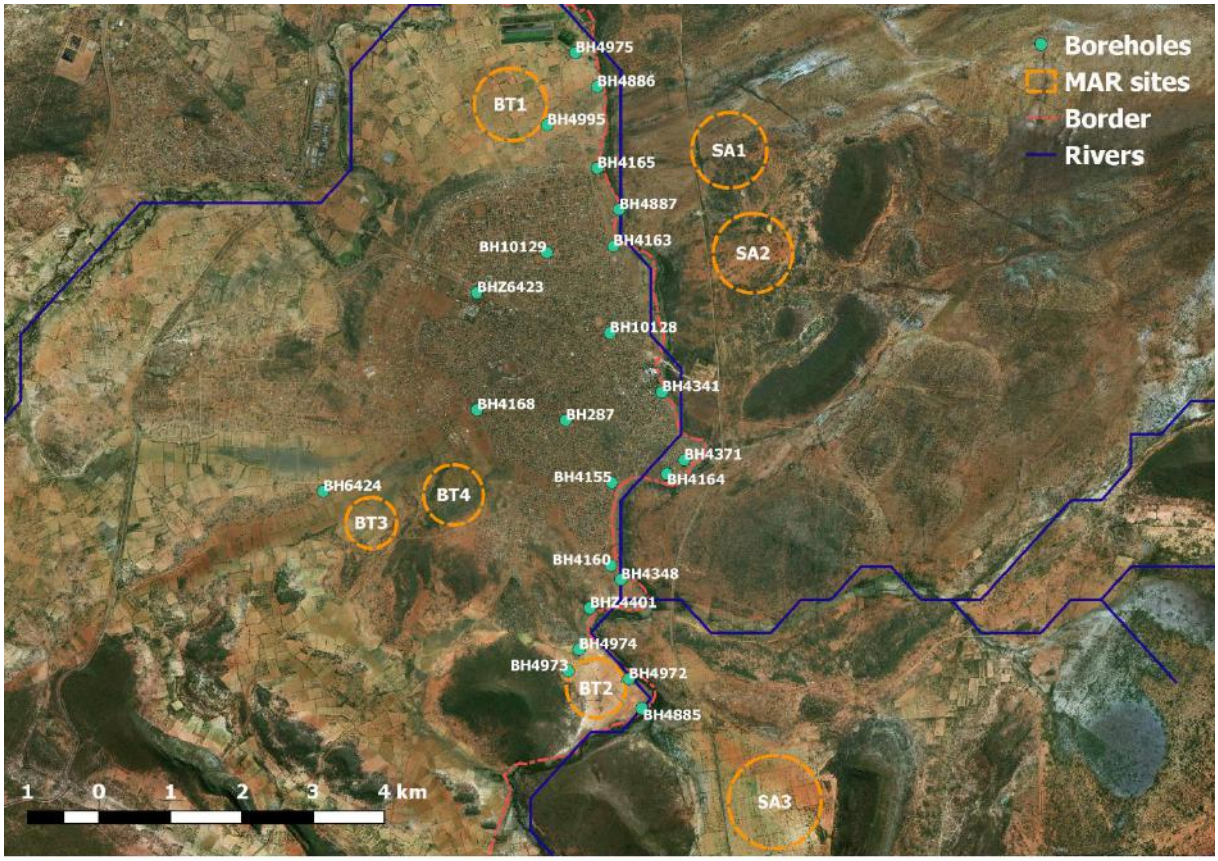

Figure 23: Possible MAR locations for surface infiltration.

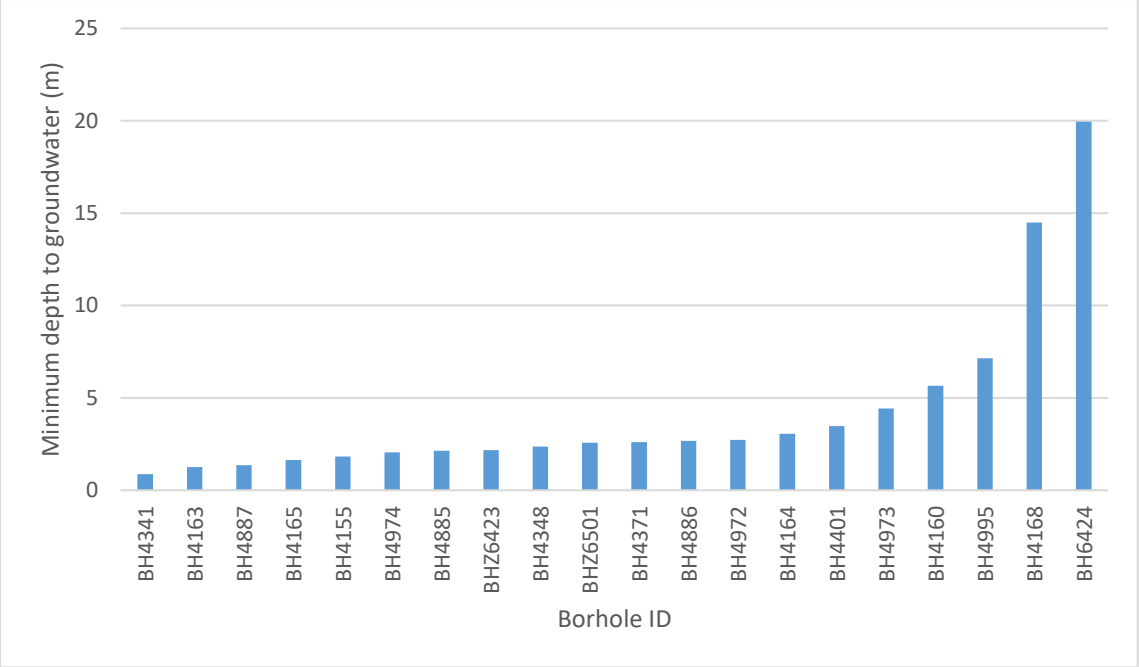

Figure 24: Minimum depth to groundwater during the period [2000-2017]

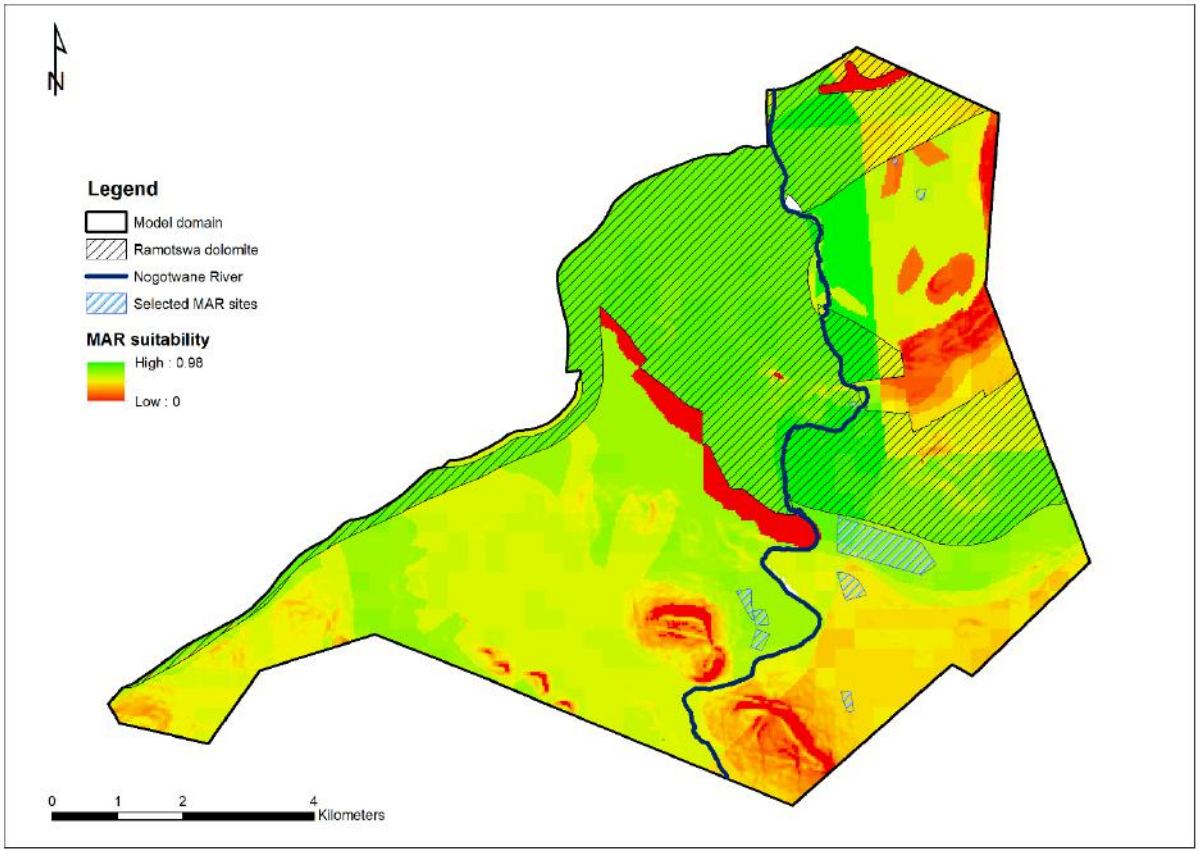

Figure 25: MAR sites suitability map and final selected sites for MAR assessment using Hydrogeological model

10. Geochemical modelling

The main objective of this section is to assess geochemical reactions of mixing of recharge water with native groundwater using geochemical model called PHREEQC. These include change in speciation and saturation indices (SI) of recharge water and ambient groundwater and other geochemical reactions such as dolomite dissolution and clogging due to precipitation of Fe(III) hydroxides. The results of the geochemical modelling help to guide source water selection and level of treatment required for MAR source water. It also provide understanding of water quality recovered from MAR operation (Vanderzalm et al., 2010). Parkhurst and Petkewich (2002) recommended that any MAR assessment should include geochemical modelling and the level of the modelling should also be appropriate to the scale of the project. Geochemical modelling usually involve significant data collection efforts (Antoniou et al., 2013), however, in the Ramotswa the available data is very limited. For the geochemical modelling, direct injection using wells is assumed, as this is the worst case scenario.

10.1 Description of PHREEQC

PHREEQC is an open source modelling program written in C and C++ programming languages. It is designed to perform solution-based geochemical calculations to simulate chemical reactions and transport processes in a user-defined system that simulates the water body. The widely applied capabilities of PHREEQC include: 1) speciation and saturation-index calculations; 2) batch-reaction and 1-dimensional transport process for both reversible and irreversible reactions, and 3) inverse modelling which accounts intermediate reactions between sets of initial and final water states. PHREEQC includes thermodynamic databases and kinetic constants for a wide range of reactions between multiple phases, e.g. aqueous, mineral, gas, solid-solution, surface complexation, ion exchange, kinetics-dependent reactions, temperature and pressure-dependent reactions and mixing of solutions with reactions (Parkhurst and Appelo, 2013).

10.2 Input data requirements and available data

Geochemical analysis should include minimally all major ions, pH and carbonate alkalinity (Davis, 1988). Analysis of trace dissolved species concentrations is necessary because these solutes often are very reactive in water-rock system. An assessment of redox condition of the aquifer requires measurement of redox-sensitive ions that occur in greatest mass (typically total dissolved ferric (Fe^{3+}) and ferrous (Fe^{2+}) iron and sulfate (SO_4^{2-}) and total dissolved sulfide (S^{2-}) concentrations) (Mirecki, 2006). It is important to ensure that charge-balance errors of samples is within ± 2% in samples where all ion concentrations have been measured. When major ion concentrations are not measured, then accurate charge-balance errors cannot be calculated, thus limiting an assessment of data quality (Mirecki, 2006).

The redox potential (Eh or pE, reported as Oxidation Reduction Potential [ORP] in millivolts) is rarely reported in the field. However, for geochemical modelling of speciation and mineral saturation is required. In addition, pH and temperature are required for mineral saturation modelling. Dissolved oxygen (DO) can be used as a proxy for Eh (Dillon et al., 2010). Estimation of the Eh/pE value can be challenging because species that quantify redox state in oxic environments (DO) sometimes are measured inaccurate in the field (non-equilibrated DO probe or exposure to air in the well bore). Species that quantify redox state in anoxic environments (sulphide/sulfate; ferrous/ferric) are often not measured during routine sampling. Furthermore, knowledge about the geological formation of

the subsurface environment, especially the mineral phases of the aquifer, is required to model water-rock interactions.

In the study area, Eh/pE data is not available for both the surface (river water) and groundwater, redox sensitive elements such as iron were measured as total concentration and it is difficult to make distinction based on their valances, bicarbonate (HCO_3^-) and nitrate were not measured in surface water samples. The pE for recharge water (river water) is calculated from the O(-2)/O(0) and used in all calculations that require a pE (distribution of redox elements and calculation of saturation indices). The concentration of O(0), dissolved oxygen was adjusted until a log partial pressure of oxygen gas of -0.7 is achieved (~20 Vol-%, atmospheric pressure), meaning that surface waters are assumed to be in equilibrium with atmospheric O_2 (Parkhurst and Appelo, 2013). HCO_3^- concentrations in surface water samples were estimated, so that the charge-balance of the surface water samples is balanced.

Groundwater samples collected in the Ramotswa do not have information regarding the redox state of the aquifer as well as DO. In recent study McGill et al. (2018) measured DO at multiple times at various boreholes in the study area (Figure 26-28). For Northern boreholes the average DO values for BH4165 (0.49 mg/l) was used to calculate the pE of the aquifer with PHREEQC. For the central boreholes average concentration of DO (2.0 mg/l), in the production borehole (BH4337) was used to determine the redox sate of the aquifer as it is close to BH4164 which was selected in the water quality analysis to represent the central part of the study area. In the southern part of the study area, average DO concentrations of production BH 4340 (1.9 mg/l) were taken to be representative for BH 6501 and to calculate the pE of the groundwater. As iron is a redox sensitive species, the estimated redox state has a large impact on the model output for dominant mineral phases influencing solution composition (Dillon et al., 2010). Due to lack of Nitrate data in the surface water samples, the fate of nitrate during MAR was not modelled.

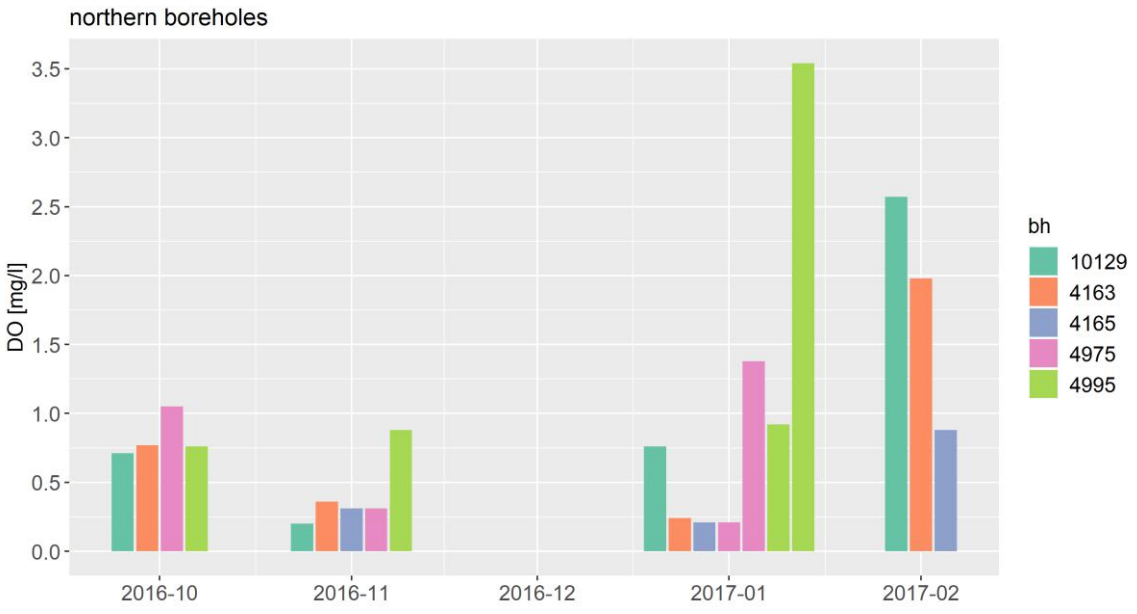

Figure 26: Dissolved oxygen (DO) in the northern part of the Ramotswa study area

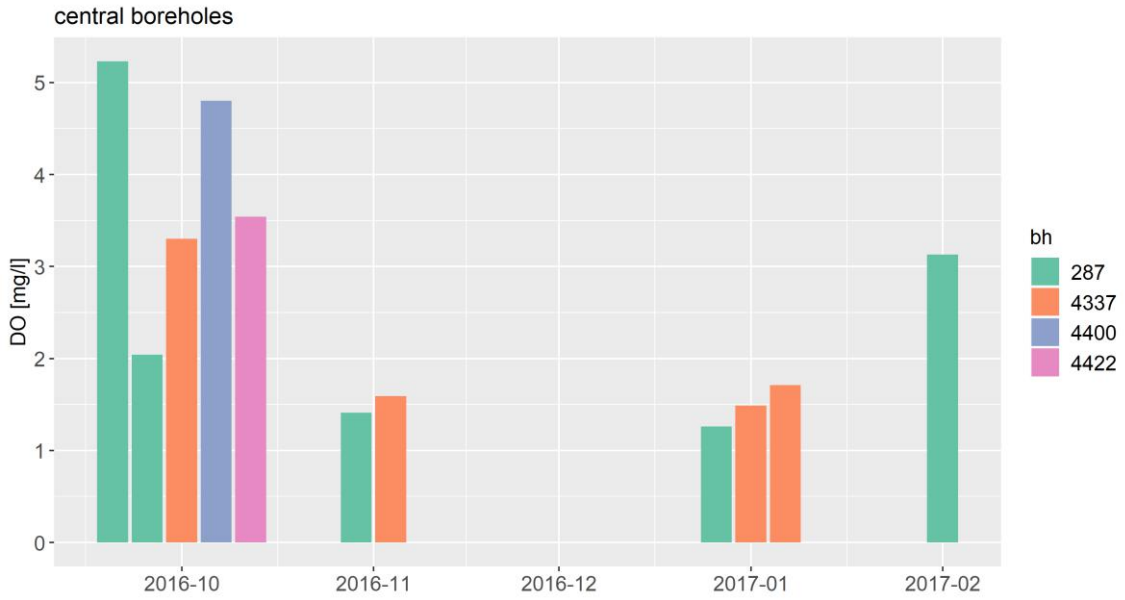

Figure 27: Dissolved oxygen (DO) in the central part of the Ramotswa study area

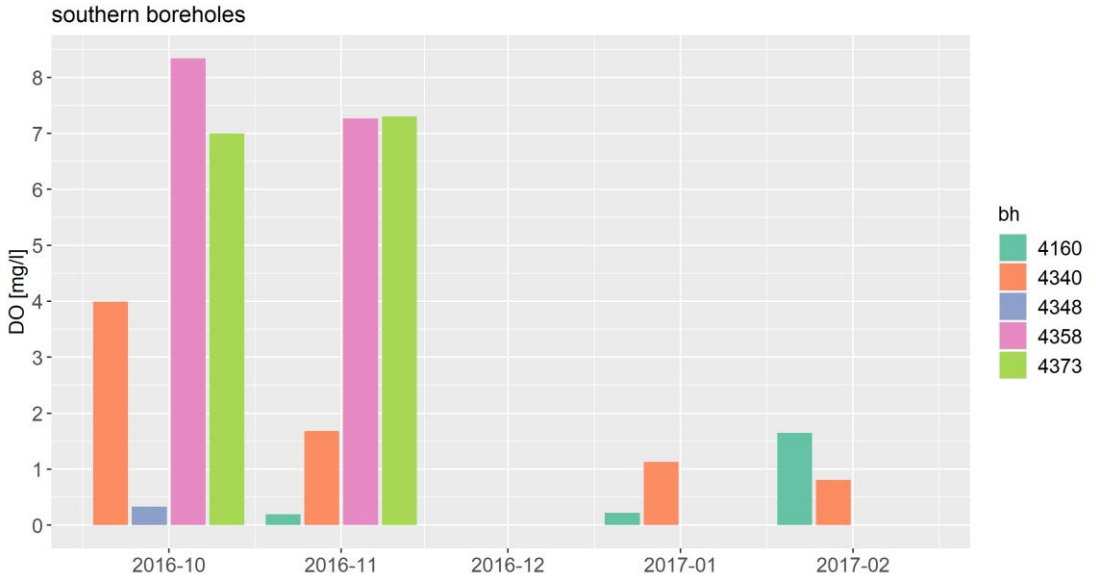

Figure 28: Dissolved oxygen (DO) in the southern part of the Ramotswa study area

10.3PHREEQC application procedure

In the present study direct injection into the aquifer was modelled as a complete mixing batch-reaction in a proximal zone of immediate mixing which develops around the injection well. Injected water is assumed to be mixed with groundwater in different proportions. We assumed four different ratios of mixing (ratios between groundwater rand injected water): mixing ratios of 80:20; 60:40; 40:60 and 20:80.

Three different sites were chosen to represent varying groundwater chemistry in the study area. Groundwater data from BH6501 was used to represent the Southern part of the study area, data from BH4164, was used to represent the central part, and data from BH4165 used to represent Northern part. The three selected regions are located in different geology. BH6501 is located in the Lepahale

formation, BH4164 is located in the dolomitic formation and BH4165 in the Black Reef Quartzite. Trace elements and redox-sensitive elements (iron, manganese etc.) were based on water quality data measured in 2004. Similarly, for the recharge water (river water) data sampled during July/August 2017 were used. The final mixtures are equilibrated with dolomite (only at BH 4164) and amorphous iron hydroxide ($Fe(OH)_3$) to simulate water-rock interactions and to assess the potential of iron clogging in the proximal zone.

The following steps were used to simulate mixing reactions in PHREEQC using the keyword data block MIX and EQUILIBRIUM_PHASES.

1 Physical and chemical characteristics of injection water are specified in SOLUTION 1
2 Composition of groundwater is defined in SOLUTION 2
3 Mixing of the two solutions in a pre-determined ratio. The keyword data block MIX performs a batch-reaction calculation reaching an equilibrium aqueous state, which can be used to mix together two or more aqueous solutions.
4 The final mixture is equilibrated with dolomite (BH 4164) and amorphous iron hydroxide using the keyword data block EQUILIBRIUM_PHASES, which defines the assemblage of pure phase in the aquifer system and performs calculations between the specified aqueous phase. Based on geological analysis of the Ramotswa aquifer, dolomite is the main relevant solid phase. Literature shows that dissolved iron precipitates initially as amorphous iron hydroxide under oxidizing conditions (Mirecki, 2006). Based on this evidence, equilibrium was modelled to assess the amount of Fe(OH)3 that could precipitate. By specifying the phases, the program extracts the chemical compositions, reaction mechanisms and thermodynamic data that are built in the database (named wateq4f).

10.4 Geochemical modelling results

Surface water sample measured at "*Ram South*" sampling point were used for geochemical modelling. The two samples were one taken on July 2017 and another on August 2017. The July and August water samples had an ionic strength of 7.23e-03 and 9.19e-03 mol/l, respectively and therefore a low mineralization. Ion strength of groundwater samples ranged from 1.25e-02 – 1.47e-02 mol /l (average mineralization). Charge-balance errors of groundwater samples were all below 2%. Bicarbonate concentrations for surface water were estimated. Geochemical modelling results of speciation of selected elements (mol /l) and saturation indices for selected minerals and gases for all three boreholes and each recharge water quality are presented in Annex 1 The saturation index for gases represents the log partial pressure (e.g. if the SI is -0.7, the partial pressure will be $10^{-0.7} = 0.1995$ $(19.95\ Vol\%)$) The lower the SI, the lower the partial pressure of the gas. Results show speciation and SI for recharge water, groundwater, and changes for each mixing ration (Mix1 – Mix4) as well as changes in speciation and SI after equilibration of each mixture with dolomite (only BH 4164) and amorphous iron hydroxide.

Saturation index (SI) is the logarithm of the quotient of the ion-activity product (IAP) and solubility-product (K_{SP}) (Equation 9). IAP is the product of element activities, which is determined by analytically measured concentrations which are transformed to activities considering ionic strength, temperature and complex formations. The solubility-product represents the maximum possible solubility at the respective water temperature and is determined from literature (Merkel et al. 2008). For example, a

value of +1 indicated a tenfold supersaturation, a value of -2 a hundredfold undersaturation in relation to a certain mineral phase.

$$SI = log \frac{IAP}{K_{SP}} \quad (9)$$

Dolomite dissolution depends very much on the composition of the recharge water, especially on the pH and pCO_2. Two different river water samples were used to model the impact of injection on the three groundwater locations. The first river water sample ("Injection1") is pH neutral (pH = 7.06), and slightly undersaturated regarding calcite (SI = -0.79) and dolomite (SI= -0.75). The second river water sample ("Injection2") is supersaturated regarding both calcite (SI=1.42) and dolomite (SI=3.63) due to the high pH of 9.67 and therefore the low pCO_2 (SI = -4.54 ~ 0.003 Vol.-%)

BH4164 is the only one situated in the Ramotswa dolomite of the selected boreholes. It is supersaturated regarding calcite (SI=0.89) and dolomite (Si= 2.31). Thus, mixed waters approach equilibrium and are even slightly undersaturated regarding calcite and dolomite at the highest mixing rations ("*Mix4*") when "*Injection1*" is used. In contrast, mixing with the already supersaturated recharge water "*Injection2*" will result in a continued increase of SI for calcite and dolomite, respectively.

The boreholes BH4165 (Ramotswa north) and BH 6501 (Ramotswa south) are both not inside the Ramotswa dolomite. However, injection of supersaturated water regarding calcite and dolomite will change the chemical composition of the groundwater, leading to a supersaturation regarding calcite and dolomite at both sites. Thus, even no carbonate rocks are present, both minerals could precipitate, especially calcite, which reaches equilibrium much quicker than dolomite

The analysis of the saturation indices for calcite and dolomite revealed that potential future dissolution of dolomite is strongly dependent on pH of the injection water. If *"Injection1"* with a neutral pH is used, supersaturated groundwater at BH 4164 approached equilibrium while recharge with "*Injection2*" would lead to supersaturation regarding calcite and dolomite at all sites, thus precipitation reactions could be possible. The supersaturated groundwater at BH 4164 regarding dolomite would approach equilibrium when "*Injection1"* is used but when an alkaline recharge water (*"Injection2"*) is used, the possible amount of precipitated dolomite even increases. However, disequilibria of dolomite can be maintained for a long time due to its inertness (Mirecki, 2006). Therefore, it is unlikely that over a period between recharge and recovery the simulated equilibrium will go to completion.

Clogging due to precipitation of Fe/Mn hydroxides As discussed in earlier sections, clogging poses a great threat to operational aspects of MAR. The most common form are iron incrustations which emerge from oxidation of reduced Fe^{2+} ions in groundwater through infiltration of oxygenated surface water. Highest iron concentrations was measured at BH 4165 and BH 6501. Concentrations at BH 4164 were low. Under the calculated redox conditions from the DO measurements, iron is predominately present as Fe(III) in the ambient groundwater, even in the north of Ramotswa (BH 4165) where oxygen concentrations are lowest. The concentrations of soluble Fe(II) is low in all groundwaters, because it is predominant under reducing conditions. The risk of clogging through MAR increases with increasing Fe(II) concentrations in ambient groundwater, because it will react with recharged oxygen-rich water and is likely to precipitate as amorphous iron hydroxide ($Fe(OH)_3$)

Groundwater at all three sites are oversaturated in amorphous iron hydroxide. A fast precipitation reaction of amorphous iron hydroxide can be anticipated why only a moderate super-saturation occurs (SI = 1.56-1.82) (Merkel et al. 2008). Therefore, the SI of $Fe(OH)_3$ was used to assess potential for iron clogging in the aquifer at the different sites. For the three boreholes sites irrespective of the injection water quality (*Injection 1 and 2*), the mixing of waters doesn't increase the SI of $Fe(OH)_3$, because the proportion of oxidizable Fe(II) in the ambient groundwaters is too low. However, all groundwater are supersaturated regarding $Fe(OH)_3$, why equilibrium was modelled to assess the potential amount that would precipitate. Unlike dolomite, the different injection water quality does not seem to influence the SI of $Fe(OH)_3$. Due to high initial concentrations of iron in groundwater, highest amount of $Fe(OH)_3$ precipitates at BH4165 why potential for geochemical clogging through iron precipitation is assumed to be highest in this area, although this would not be due to MAR but to the ambient groundwater quality.

11 MAR potential assessment using Hydrogeological model

11.1 Hydrogeological model description

A hydrogeological model was developed for the Ramtoswa Aquifer for the period 2000-2017. The model was developed using MODFLOW-2005. A transient 3-dimensional groundwater flow model was constructed in MODELMUSE modelling environment using MODFLOW-2005. The model was discretized horizontally into a 90 m x 90 m uniform grid, and vertically into two layers representing the upper and deeper karstic layers respectively. Dykes that were thought to act as lateral flow barriers were simulated in the model. Abstraction for 9 public supply wells were determined from data supplied by Water Utility cooperation, Botswana. The model was calibrated to simulate the groundwater levels for 2000-2012, and validated using measured levels during the period of 2015-2017. Spatially averaged diffuse recharge was estimated using by multiplying monthly rainfall by multiplier constant, which was determined using model calibration. The model was calibrated using PEST, automatic calibration algorithm using water level data in 17 observation wells. The calibrated and validated hydrogeological model was used to evaluate the feasibility of MAR in the aquifer.

11.2 Description of simulation-optimization model

When a simulation model is used alone for developing groundwater management strategies, it often requires a time consuming, iterative trial-and-error approach. When using trial and error, the results are also, to some extent, subjective, because only a limited number of management alternatives can be tested. However, in the optimization approach precise numerical criteria are used to specify the limit of acceptability of management alternatives.

In the present study the Ground-Water Management software package GWM (Ahlfeld et al., 2005) was used to formulate the optimization problem and to identify optimal rate of MAR. GWM-2005 is a three-dimensional groundwater flow simulation coupled groundwater optimization model. In GWM optimization process consists of defining the objective function, decision variables and a set of constraints. A single objective function is supported by GWM which can be specified to either minimize or maximize the weighted sum of the three types of decision variables.

GWM uses the well-known Response Matrix Solution approach to calculate the change in head at each constraint location that results from the perturbation of a flow rate variable; these changes are used

to calculate the response coefficients. The response matrix technique utilizes superposition and linear systems theory to simulate groundwater flow (Gorelick et al., 1993; Peralta et al., 1991). A response matrix consists of linear influence coefficients that describe the response of hydraulic head to a unit volume of extraction or injection of groundwater. These coefficients are termed response functions. The hydraulic head response matrix is formed by running the simulation model once for each injection or pumping well. This helps to obtain hydraulic heads at each control points as a linear combination of the injection or pumping rates. The response function can be solved using the linear programing (LP) or successive linear programming (SLP) solution algorithm. The SLP algorithm is computationally more intensive than LP because the Jacobian matrix needs to be recomputed at each iteration of the algorithm. But, it is good to solve non-linear problem (notably flow in unconfined aquifers). The LP algorithm is applicable to linear problems (e.g. confined aquifers). In this study we used LP solution algorithm mainly due to low computational requirement.

11.3 Infiltration basin

For the scenario assessment using the hydrogeological model an active infiltration area of 1 ha was assumed. The grid size used in the numerical model dictate the choice of the infiltration basin area. The larger the infiltration area, the lower the magnitude of groundwater mounding as the infiltration is dispersed over a wider area. The infiltration rate determined using infiltration test is assumed to be equal to recharge. The infiltration rate is assumed to be constant over time and the infiltrated water reaches the water table instantly, hence the effect of unsaturated zone is neglected. In reality several factors change the rate of infiltration with time, one of which is clogging. Normally, within several week to several months, the infiltration rate reaches a low but fairly constant rate called the basic infiltration rate (Zomorodi, 1991). Two methods exist to simulate infiltration from the infiltration basin. The first option is to use recharge package and specify recharge as m/d. The second, is using Well package and specify the infiltration rate as volume per day by multiplying with area. Although, the two methods will lead to the same solution, Well package provide some flexibility in its applications. Hence, following the methodology by Woolfenden and Koczot (2001) infiltration from the infiltration basin is represented using the Well package.

11.4 Recharge volume

The GWM model was designed to solve aquifer recharge for wet and dry years. The year 2009 with annual rainfall of 903 mm/a was selected to represent the wet year and year 2017 with annual rainfall of 157 mm/a represents below average or dry year. The three month period [January- March] was selected as a recharge period. The optimization model was designed to maximize the total quantity of recharged water during the three month while satisfying water level constraint to prevent groundwater mounding. As described above recharge from infiltration ponds were simulated using well package. Hence, require the specification of injection rates at each candidate sites. The objective function of for each year recahrge is written as Equation 10.

$$Maximize \ \sum_{n=1}^{N} QT_{Qn} \qquad (10)$$

Where:

Q is injection flow rate at managed well site, N is total number of injection wells, and T_{Qn} is the total duration of injection at well site.

The number and location of potential infiltration basin sties were fixed based on MAR suitability mapping and additional criteria such as water quality issues and depth to groundwater. The decision variables are rate of injection wells. The constraints are: (1) groundwater level limited to 3 m below the ground surface (assuming 2 m depth infiltration pond and allowing additional 1 m below the infiltration basin to avoid reduction in the infiltration rate); (2) the lower and upper bound of the injection constraints. The upper bound for each injection wells were determined by multiplying infiltration rate determined using double ring infiltrometer by gird area, and the lower bound was set to zero. The total volume of water injected per day for three month period for dry and wet year is presented in Table 8. The total volume of water injected into the aquifer in three months period [Jan-March] during the dry period in Botswana is 1920 m^3/d (**0.172 x 10^6 m^3**) and in South Africa is 6540 m^3/d (**0.589 x 10^6 m^3).**

Table 8: Optimal recharge volumes, soil infiltration rate is the infiltration rate determined using double ring infiltrometer. For Botswana side the average infiltration rate at site 6 and 7 was used and in South African side soil infiltration rate average at site 14 and 15 was used.

Infiltration basin name	X	Y	Elevation	Soil infiltration rate (m/d)	Injection rate (m^3/d)	
					2009	2017
BS1	386180.99	7243779.40	1031.615	2.817	212.00	494.00
BS2	386178.15	7243943.70	1031.851	2.817	187.00	391.00
BS3	386166.83	7244141.90	1031.851	2.817	228.00	440.00
BS4	386166.83	7244328.80	1030.198	2.817	62.40	353.00
BS5	385999.02	7244408.5	1029.844	2.817	51.80	241.00
BS6	386002.56	7244585.20	1027.954	2.817	0.00	0.00
Total					**741.00**	**1920.00**
SA1	387531.93	7244593.70	1036.928	6.552	918.00	1200.00
SA2	387529.10	7244773.50	1037.282	6.552	996.00	1260.00
SA3	387434.93	7245219.9	1027.128	6.552	61.90	328.00
SA4	387434.93	7245590.9	1029.371	6.552	616.00	932.00
SA5	388516.82	7244848.9	1036.928	6.552	1010.00	1420.00
SA6	388519.65	7245217.1	1036.102	6.552	997.00	1400.00
Total					**4600.00**	**6540.00**

11.5 Travel time assessment

Particle tracking simulations were performed to evaluate the residence time of infiltrated water before it is recovered with existing production boreholes (Figure 29). The particle tracking with performed using MODPATH (Pollock, 1994), a post-processing program for MODFLOW-2000. MODPATH computes particle paths using a semi-analytical expression of the flow path of a particle within each cell and tracks the movement of the particle from one cell to the next until the particle is terminated at a boundary, an internal sink or source, or some other user-defined criterion. Particles were placed at the infiltration basin and tracked forward. The time it takes for the fastest particle to reach the pumping wells were calculated. Results of particle tracking shows that none of the production borehole capture injected water less than 60 days old, as regulatory limit required for inactivation of pathogens or other nutrients commonly present in treated wastewater.

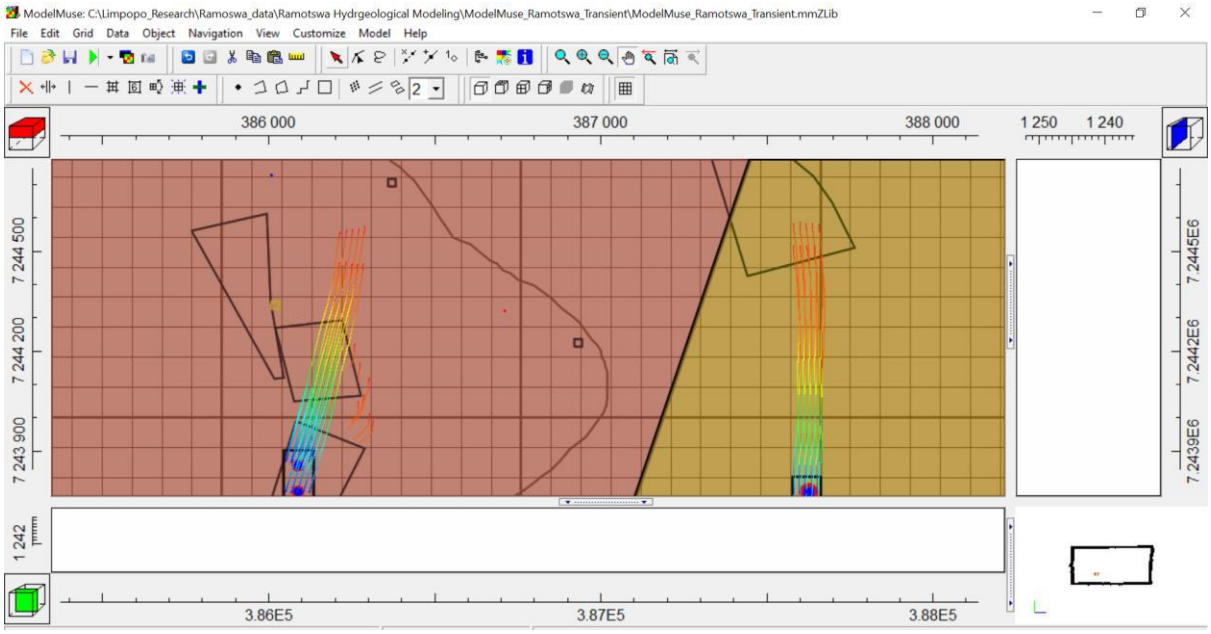

Figure 29: Forward particle tracking from the MAR recharge sites. The small rectangles shown along the river are existing production boreholes.

12 Discussion

Water quality Groundwater quality in the Ramotswa is highly variable both spatially and temporally. Water quality assessment showed that high nitrate concentrations remain a problem in the Ramotswa wellfields, which are likely to be associated with leaching from pit latrines, septic tanks as well as fertilizers. Additionally, very high iron (and manganese) concentrations have been observed at several boreholes in the study area. High Fe or Mn concentrations in groundwater could pose clogging problem and affect MAR operation. The main challenge remains the lack of data in sufficient quantity and quality. No data was available on microbial risks or faecal coliforms, which must be considered when pollution from pit latrines or septic tanks is assumed. Furthermore, no data about disinfection by-products, pharmaceuticals or radionuclide are available, which are found to be important parameter to consider in a similar

Water source availability possible water sources for MAR were investigated to assess the amount of water available for MAR. Excess water from floods in the ephemeral Ngotwane River during the wet season is a likely source for MAR, but quantitative assessment was challenging due to the lack of runoff data. The main source of water for MAR for the Ramotswa Transboundary is the the Ngotwane/Notwane ephemeral River. The period between November- March has good rainfall (above 50 mm/month) hence may provide good runoff that can used for MAR. However, there are concerns about diversion of the Ngotowane River flow for MAR that may reduce water now available for storage downstream in the Gaborone dam (Mosses, oral communcation). The Kharkams, case study South Africa (Murray and Tredoux, 2002), provide a good example where empheral flow is diverted using intake structure and used for MAR via injection wells. Other potential sources of water for recharge include wastewater from the Ramotswa village. The advantage of considering wastewater as a source is its availability throughout the year irrespective of the rainy season. The downside is that it required extensive pre-post-treatment and it would be very costly.

Geochemical modelling Geochemical modelling was used to assess the risk of chemical clogging through iron hydroxide precipitation and further dolomite dissolution when waters of different

chemical compositions are mixed during MAR. Results shows that further dolomite dissolution is unlikely, especially when alkaline recharge water is used, although processed that further increase acidity in the aquifer, like organic matter oxidation, couldn't be considered in the simplified modelling approach. Iron is predominantly present as Fe(III) because oxygen remained at least in small concentrations in the analysed groundwater samples. Furthermore, precipitation of iron hydroxides through the injection of oxygen rich water in the aquifer is unlikely, because most parts of the aquifer are not anoxic and thus the proportion of soluble, oxidizable Fe(II) is low. However, high iron concentrations with still favour bacterial growth and clogging through biofouling, as it was observed by a WUC study in 2015 at multiple production boreholes in Ramotswa.

Potential MAR sites Based on literature review and availability of data, Ebrahim et al.(2017) used four criteria; lithology, soil, slope and land use and land cover and developed MAR suitability map for the Ramotswa area. In the present study additional data which are not included in the multi-criteria analysis due to limited spatial coverage was included in the screening of potential MAR sites. The zonal approach was used in the criteria assessment. Meaning, representative potential zones from the suability map were selected and analysed based on addition criteria. The additional criteria used in further screening of potential MAR sites were: water quality, depth to groundwater, soil infiltration test conducted during this study. Most of the information except soil infiltration test which was conducted in both countries, most of the other information such as depth to groundwater, water quality is only available from the Botswana side of the study area. However, inference of water quality in South Africa side was made based on land use. Based on additional criteria assessment potential sites in the South of the study area were selected. The two sites are located outside of the dolomite formation.

Aquifer storage capacity Aquifer storage potential during the three month time [January- March] was determined for very wet and dry years, year 2009 and 2017 respectively. During the very wet year the minimum depth to groundwater along the river channel in the Botswana side is within 1-2 m below ground surface. Since, no data is avialble in the South African side the minimum depth to groundwater is unknown. The optimization problem found optimal solution in five out of the six MAR sites. The optimization problem could not found optimal solution in site 6 in the Botswana side. This is because depth to groundwater is less than 3 m defined as head constraint for groundwater level rise (mounding). The total recharge volume in the five MAR sites is about 7.418 x 10^2 m^3/d (0.06 x 10^6 m^3 for the three month period).The total volume of water that can be stored during the same period in South African side was found to be 4.597 x10^3 m^3/d (0.414 X10^6 m^3 for the three month). The total recharge volume during the dry year in the South Africa side is about 6.541 x 10^3 m^3/d (0.589 x 10^6 m^3 over the three month period). Similarly, the total volume of water recharged into the aquifer in the Botswana side is about 1.919 x 10^3 m^3/d (0.172 x 10^6 m^3 over the three month period).

To obtain the infiltration rate basin area divide the total injection rates by soil infiltration rate. It is important to note that the infiltration rate will reduce over time due to clogging. Furthermore the rate of infiltration will also be affected by water depth in the infiltration rate, which is not accounted in the present analysis.

13 Conclusions

A hydrogeological modelling approach was used to investigate the feasibility of MAR in the Ramotswa Transboundary Aquifer Area. A 3D transient hydrogeological model based on MODFLOW 2005 was used in conjunction with GWM 2005 and particle tracking algorithm (MODPATH). Based on MAR suitability mapping and additional criteria such as water quality and depth to groundwater potential MAR sites were identified for each countries. From each country six potential infiltration basin sites were selected from the potential MAR sites. The optimization problem involves maximization of groundwater recharge during the three month period [January – March] given groundwater level constraint. Two optimization problems were formulated; for wet (year 2009) and dry (2017) years. The total recharge volume during the dry year in the South Africa side is about 6.541 x 10^3 m^3/d (0.589 x 10^6 m^3 over the three month period). Similarly, the total volume of water recharged into the aquifer in the Botswana side is about 1.919 x 10^3 m^3/d (0.172 x 10^6 m^3 over the three month period). However, the total recharge volume decrease during the wet season due to raise in groundwater levels. During high/good rainfall years the aquifers get saturated with natural recharge, leaving little storage space for MAR. Water budget and water level analysis after three month recharge period has shown that there is little scope for the stored water to stay in the aquifer for subsequent recovery during the dry period. It is important to note that due to shallow depth to groundwater the stored water is lost through evapotranspiration directly from the groundwater. In this case immediate pumping, after recharge (e.g. April, within one month after recharge) would be needed to optimize recharge water.

The water quality characterization results shows high spatial variability in water quality. High Nitrate is the main problem in Ramotswa. However, since the selected MAR sites are far from the town MAR operation is less affected Nitrate contamination. The Geochemical modelling results confirm no further dolomite dissolution due to MAR. However, as already observed in the Ramotswa production boreholes the issue of iron incrustation (clogging) still be a problem

References

Ahlfeld, D. P., Barlow, P. M., and Mulligan, A. E., 2005, GWM--A ground-water management process for the US Geological Survey modular ground-water model (MODFLOW-2000), US Department of the Interior, US Geological Survey.

Antoniou, E., Stuyfzand, P., and van Breukelen, B., 2013, Reactive transport modeling of an aquifer storage and recovery (ASR) pilot to assess long-term water quality improvements and potential solutions: Applied geochemistry, v. 35, p. 173-186.

Applin, K. R., and Zhao, N., 1989, The kinetics of Fe (II) oxidation and well screen encrustation: Groundwater, v. 27, no. 2, p. 168-174.

Arthur, J., Dabous, A., and Cowart, J., 2005, Water–rock geochemical considerations for aquifer storage and recovery: Florida case studies: Developments in Water Science, v. 52, p. 327-339.

BOS, 2000, Botswana Bureau of Standards (BOS) Water quality - Drinking water - Specification. BOS 32. Garbarone.

Catuneanu, O., and Eriksson, P. G., 1999, The sequence stratigraphic concept and the Precambrian rock record: an example from the 2.7–2.1 Ga Transvaal Supergroup, Kaapvaal craton: Precambrian Research, v. 97, no. 3-4, p. 215-251.

CSO, 2009, Botswana Water Statistics published by The Central Statistics Office (CSO)

Daher, W., Pistre, S., Kneppers, A., Bakalowicz, M., and Najem, W., 2011, Karst and artificial recharge: Theoretical and practical problems: A preliminary approach to artificial recharge assessment: Journal of Hydrology, v. 408, no. 3-4, p. 189-202.

Davis, S. N., 1988, Where are the rest of the analyses?: Groundwater, v. 26, no. 1, p. 2-5.

Dillon, P., Pavelic, P., Page, D., Miotlinski, K., Levett, K., Barry, K., Taylor, R., Wakelin, S., Vanderzalm, J., and Molloy, R., 2010, Developing Aquifer Storage and Recovery (ASR) Opportunities in Melbourne—Rossdale ASR Demonstration Project Final Report: WfHC Report to Smart Water Fund, June.

Ebrahim, G. Y., Fathi, S., Lautze, J., Ansems, N., Villholth, K. G., Nijsten, G.-J., Magombeyi , M., Mndaweni, S., Kenabatho, P., Moehadu, M., Keodumetse, K., Gomo, M., Somolekae, B., Nkile, C., and Kealeboga, D., 2017, Review of Managed Aquifer Recharge (MAR) Experience in Africa and MAR Suitability Mapping for Ramotswa Transboundary Aquifer Area. International Water Management Institute.

Ebrahim, G. Y., Jonoski, A., Al-Maktoumi, A., Ahmed, M., and Mynett, A., 2015, Simulation-optimization approach for evaluating the feasibility of managed aquifer recharge in the Samail lower catchment, Oman: Journal of Water Resources Planning and Management, v. 142, no. 2, p. 05015007.

Edmunds, W., Shand, P., Hart, P., and Ward, R., 2003, The natural (baseline) quality of groundwater: a UK pilot study: Science of the Total Environment, v. 310, no. 1-3, p. 25-35.

Flint, A. L., and Ellett, K. M., 2004, The role of the unsaturated zone in artificial recharge at San Gorgonio Pass, California: Vadose Zone Journal, v. 3, no. 3, p. 763-774.

Ford, D., and Williams, P. D., 2013, Karst hydrogeology and geomorphology, John Wiley & Sons.

Gale, I., 2005, Strategies for Managed Aquifer Recharge (MAR) in semi-arid areas, UNESCO.

Ganot, Y., Holtzman, R., Weisbrod, N., Nitzan, I., Katz, Y., and Kurtzman, D., 2017, Monitoring and modeling infiltration-recharge dynamics of managed aquifer recharge with desalinated seawater: Hydrology & Earth System Sciences, v. 21, no. 9.

Ghasemizadeh, R., Hellweger, F., Butscher, C., Padilla, I., Vesper, D., Field, M., and Alshawabkeh, A., 2012, Review: Groundwater flow and transport modeling of karst aquifers, with particular reference to the North Coast Limestone aquifer system of Puerto Rico: Hydrogeology journal, v. 20, no. 8, p. 1441-1461.

Gorelick, S. M., Freeze, R. A., Donohue, D., and Keely, J. F., 1993, Groundwater contamination: optimal capture and containment, Lewis Publishers Inc.

Green, R. T., Painter, S. L., Sun, A., and Worthington, S. R., 2006, Groundwater contamination in karst terranes: Water, Air, & Soil Pollution: Focus, v. 6, no. 1-2, p. 157-170.

Hengl, T., de Jesus, J. M., Heuvelink, G. B., Gonzalez, M. R., Kilibarda, M., Blagotić, A., Shangguan, W., Wright, M. N., Geng, X., and Bauer-Marschallinger, B., 2017, SoilGrids250m: Global gridded soil information based on machine learning: PLoS one, v. 12, no. 2, p. e0169748.

Herczeg, A. L., Rattray, K. J., Dillon, P. J., Pavelic, P., and Barry, K. E., 2004, Geochemical processes during five years of aquifer storage recovery: Groundwater, v. 42, no. 3, p. 438-445.

Herman, J. S., and White, W. B., 1985, Dissolution kinetics of dolomite: effects of lithology and fluid flow velocity: Geochimica et Cosmochimica Acta, v. 49, no. 10, p. 2017-2026.

Houben, G., 2003, Iron oxide incrustations in wells. Part 1: genesis, mineralogy and geochemistry: Applied Geochemistry, v. 18, no. 6, p. 927-939.

Hsieh, H.-H., Lee, C.-H., Ting, C.-S., and Chen, J.-W., 2010, Infiltration mechanism simulation of artificial groundwater recharge: a case study at Pingtung Plain, Taiwan: Environmental Earth Sciences, v. 60, no. 7, p. 1353-1360.

Izbicki, J. A., Flint, A. L., and Stamos, C. L., 2008, Artificial recharge through a thick, heterogeneous unsaturated zone: Groundwater, v. 46, no. 3, p. 475-488.

Jiang, Y., Wu, Y., Groves, C., Yuan, D., and Kambesis, P., 2009, Natural and anthropogenic factors affecting the groundwater quality in the Nandong karst underground river system in Yunan, China: Journal of contaminant hydrology, v. 109, no. 1-4, p. 49-61.

Jones, A., Breuning-Madsen, H., Brossard, M., Dampha, A., Deckers, J., Dewitte, O., Gallali, T., Hallett, S., Jones, R., and Kilasara, M., 2013, Soil atlas of Africa.

Jonoski, A., Zhou, Y., Nonner, J., and Meijer, S., 1997, Model-aided design and optimization of artificial recharge-pumping systems: Hydrological sciences journal, v. 42, no. 6, p. 937-953.

Langmuir, D., 1997, Aqueous environmental, Prentice Hall.

López, F. V., 2017, MAR site selection in Western Europe and comparison with other suitability maps by means of the MAR index Master Thesis Master in Hydro Science and Engineering, Dresden University of Technology Department of Hydrosciences, Institute of Waste Management and Circular Economy.

Mansouri, B. E., and Mezouary, L. E., 2015, Enhancement of groundwater potential by aquifer artificial recharge techniques: an adaptation to climate change: Proceedings of the International Association of Hydrological Sciences, v. 366, p. 155-156.

Martin, N., 2017, Assessing wastewater and sanitation conditions and management in the Ramotswa Transboundary Aquifer Area between South Africa and Botswana. Promotion, Paris.

Martin, R., 2013, Clogging issues associated with managed aquifer recharge methods: IAH Commission on Managing Aquifer Recharge.

McGill, B. M., Altchenko, Y., K.;, K. P., Sylvester, S. R., and Villholth, K., 2018, Climate change, sanitation, and groundwater quality: A CHANS case study from Ramotswa, Botswana. In: Hydrogeology Journal.

Medina, D. A. B., van den Berg, G. A., van Breukelen, B. M., Juhasz-Holterman, M., and Stuyfzand, P. J., 2013, Iron-hydroxide clogging of public supply wells receiving artificial recharge: near-well and in-well hydrological and hydrochemical observations: Hydrogeology journal, v. 21, no. 7, p. 1393-1412.

Mirecki, J. E., 2006, Geochemical Models of Water-Quality Changes during Aquifer Storage Recovery (ASR) Cycle Tests, Phase 1: Geochemical Models Using Existing Data: ENGINEER RESEARCH AND DEVELOPMENT CENTER VICKSBURG MS ENVIRONMENTAL LAB.

Moral, F., Cruz-Sanjulián, J., and Olías, M., 2008, Geochemical evolution of groundwater in the carbonate aquifers of Sierra de Segura (Betic Cordillera, southern Spain): Journal of hydrology, v. 360, no. 1-4, p. 281-296.

Murray, E., and Tredoux, G., 2002, Pilot artificial recharge schemes: testing sustainable water resource development in fractured aquifers: Report to the Water Research Commission, WRC Report, no. 967/1, p. 02.

Parkhurst, D. L., and Appelo, C., 2013, Description of input and examples for PHREEQC version 3: a computer program for speciation, batch-reaction, one-dimensional transport, and inverse geochemical calculations: US Geological Survey, 2328-7055.

Parkhurst, D. L., and Petkewich, M. D., Geochemical modeling of an aquifer storage recovery experiment, Charleston, South Carolina, *in* Proceedings US Geological Survey Artificial Recharge Workshop Proceedings, April 2-4, 2002, Sacramento, California2002, p. 38.

Pavelic, P., Dillon, P. J., Barry, K. E., Vanderzalm, J. L., Correll, R. L., and Rinck-Pfeiffer, S. M., 2007, Water quality effects on clogging rates during reclaimed water ASR in a carbonate aquifer: Journal of Hydrology, v. 334, no. 1-2, p. 1-16.

Peralta, R. C., Azarmnia, H., and Takahashi, S., 1991, Embedding and Response Matrix Techniques for Maximizing Steady-State Ground-Water Extraction: Computational Comparison: Ground Water, v. 29, no. 3, p. 357-364.

Ralph, D. E., and Stevenson, J. M., 1995, The role of bacteria in well clogging: Water Research, v. 29, no. 1, p. 365-369.

Ranganai, R. T., Gotlop-Bogatsu, Y., Maphanyane, J., and Tladi, B., 2001, Hydrochemical and Geophysical Evaluation of Groundwater Pollution in the Ramotswa Wellfield, SE Botswana: BIE2001 Technical Papers, p. 193-200.

Smith, A., and Pollock, D., 2010, Artificial recharge potential of the Perth region superficial aquifer: Lake Preston to Moore River, CSIRO: Water for a Healthy Country Research Flagship.

SOLOVEY, T., and JÓŹWIAK, K., 2008, Application of geochemical modeling for analysis of changes in groundwater chemistry in karst area (case study from gypsum karst in the Czarny Potok Valley, SW Ukraine): W: Methods of landscape research, J. Pilt, V. Andrejczuk (ed.). Prace Komisji Krajobrazu Kulturowego PTG, no. 8, p. 231-243.

Sundaram, B., Feitz, A., de Caritat, P., Plazinska, A., Brodie, R. S., Coram, J., and Ransley, T., 2009, Groundwater sampling and analysis–a field guide: Geoscience Australia, Record, v. 27, no. 95, p. 104.

Valdes, D., Dupont, J.-P., Laignel, B., Ogier, S., Leboulanger, T., and Mahler, B. J., 2007, A spatial analysis of structural controls on Karst groundwater geochemistry at a regional scale: Journal of hydrology, v. 340, no. 3-4, p. 244-255.

Vanderzalm, J., Page, D., Barry, K., and Dillon, P., 2010, A comparison of the geochemical response to different managed aquifer recharge operations for injection of urban stormwater in a carbonate aquifer: Applied Geochemistry, v. 25, no. 9, p. 1350-1360.

White, W. B., 1988, Geomorphology and hydrology of karst terrains, Oxford university press New York.

WHO, 2003a, Chloride in Drinking-water. Background document for development WHO Guidelines for Drinking-water quality. Geneva, Switzerland: World Health Organization.

-, 2003b, Iron in Drinking-water. Background document for development of WHO guidelines for Drinking-water Quality. Geneva, Switzerland: World Health Organization.

-, 2003c, Sodium in Drinking-water. Background document for development WHO Guidelines for Drinking-water quality. Geneva, Switzerland: World Health Organization.

-, 2004, Sulphate in Drinking-water. Background document for development of WHO guidelines for Drinking-water Quality. Geneva, Switzerland: World Health Organization. .

-, 2009, Calcium and magnesium in drinking-water. Public health significance. Geneva, Switzerland: World Health Organization..

-, 2011a, Manganese in Drinking-water. Background document for development of WHO guidelines for Drinking-water Quality. Geneva, Switzerland.

-, 2011b, Nitrate and Nitrite in Drinking-water. Background document for development of WHO guidelines for Drinking-water Quality. Geneva, Switzerland: World Health Organization.

Williams, P. W., 2008, The role of the epikarst in karst and cave hydrogeology: a review: International Journal of Speleology, v. 37, no. 1, p. 1.

Woolfenden, L. R., and Koczot, K. M., 2001, Numerical simulation of ground-water flow and assessment of the effects of artificial recharge in the Rialto-Colton Basin, San Bernardino County, California, US Department of the Interior, US Geological Survey.

Xanke, D.-G. J., 2017, Managed aquifer recharge into a karst groundwater system at the Wala reservoir, Jordan.

Xu, Y., Shu, L., Zhang, Y., Wu, P., Atlabachew Eshete, A., and Mabedi, E. C., 2017, Physical Experiment and Numerical Simulation of the Artificial Recharge Effect on Groundwater Reservoir: Water, v. 9, no. 12, p. 908.

Zhu, N., 2013, Geochemical modeling of an aquifer storage and recovery project in Union County, Arkansas: Massachusetts Institute of Technology.

Annex 1: Geochemical modelling results

Mineral saturation index is an index showing whether a water will tend to dissolve or precipitate a particular mineral. Its value is negative when the mineral may be dissolved, positive when it may be precipitated, and zero when the water and mineral are at chemical equilibrium.

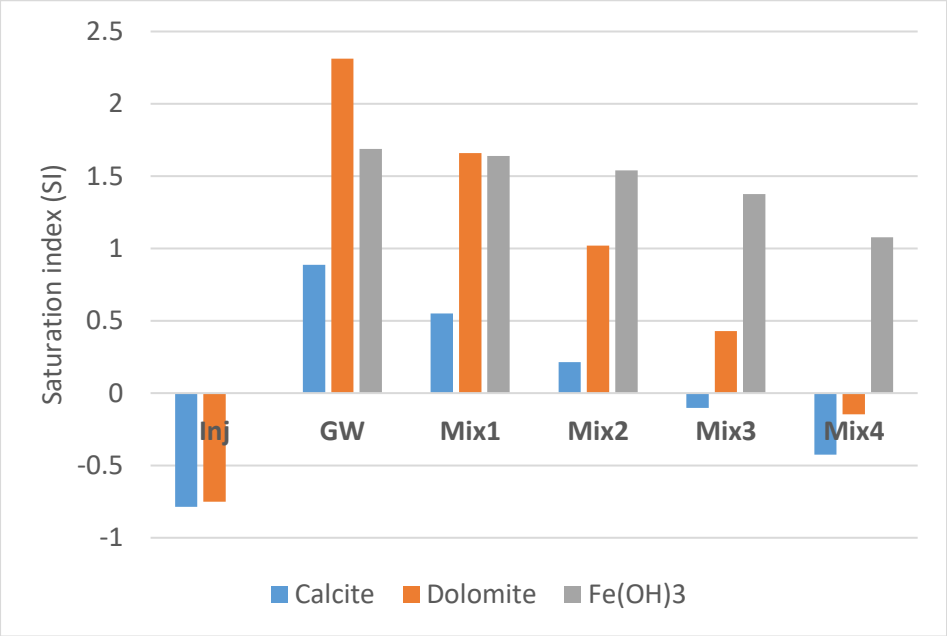

Figure1: BH4164 *- saturation indices for calcite, dolomite and amorphous iron hydroxide. Mixing proportions: Mix1 = 80% GW:20% Injection; Mix2 = 60% GW:40% Injection; Mix3 = 40% GW:60% Injection; Mix4 = 20% GW:80% Injection. Calculated with* ***injection water analysis 1*** *(Surface water sample July 2017)*

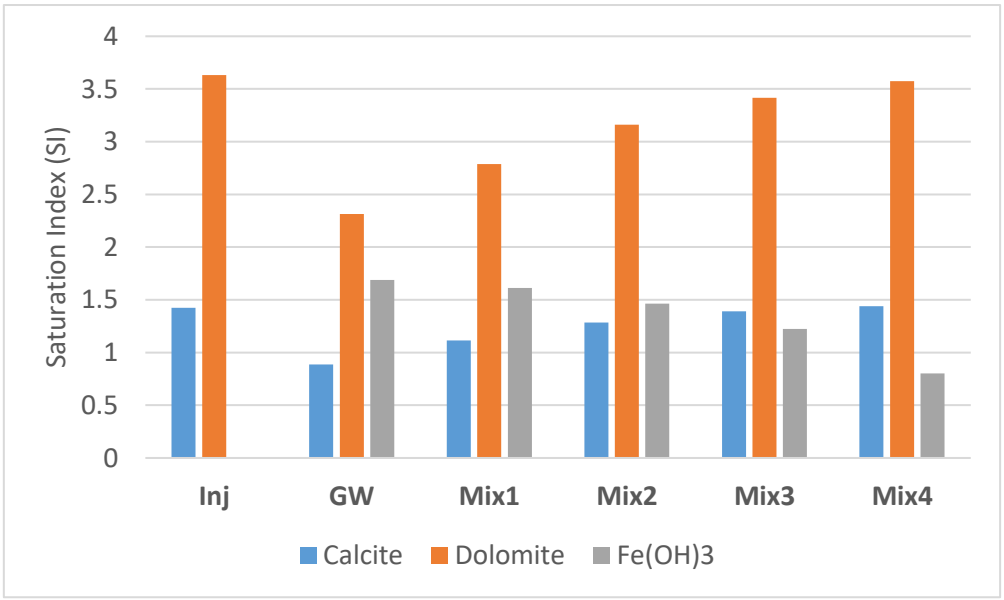

Figure 2: BH4164 *- saturation indices for calcite, dolomite and amorphous iron hydroxide. Mixing proportions: Mix1 = 80% GW:20% Injection; Mix2 = 60% GW:40% Injection; Mix3 = 40% GW:60% Injection; Mix4 = 20% GW:80% Injection. Calculated with* ***injection water analysis 2.*** *(Surface water sample August 2017)*

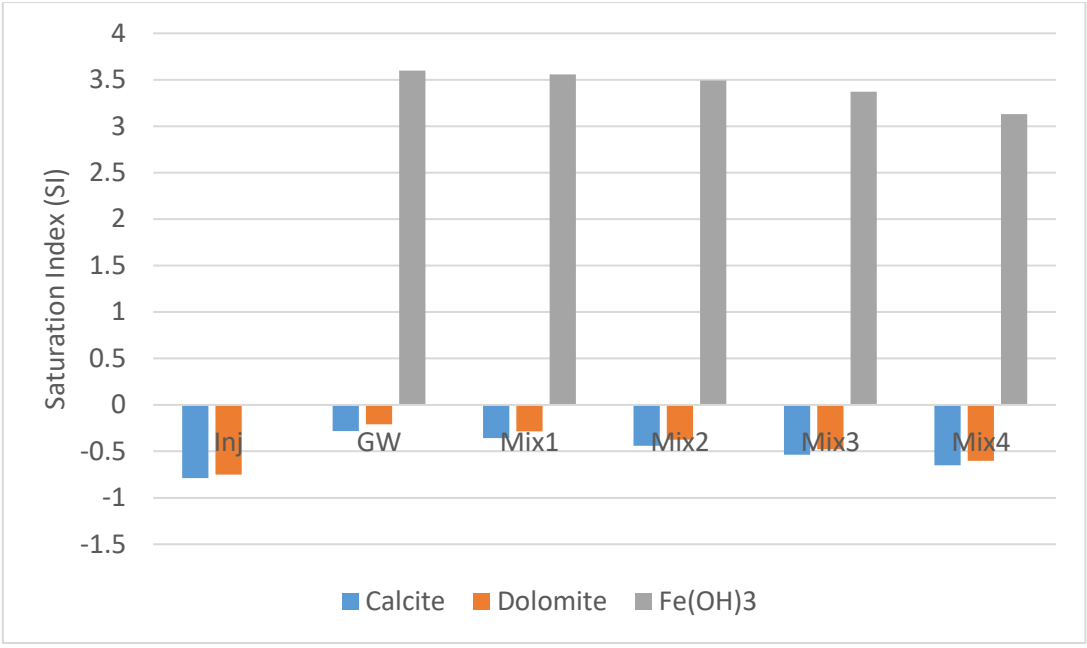

Figure 3: BH4165 *- saturation indices for calcite, dolomite and amorphous iron hydroxide. Mixing proportions: Mix1 = 80% GW:20% Injection; Mix2 = 60% GW:40% Injection; Mix3 = 40% GW:60% Injection; Mix4 = 20% GW:80% Injection. Calculated with* ***injection water analysis 1****(Surface water sample July 2017)*

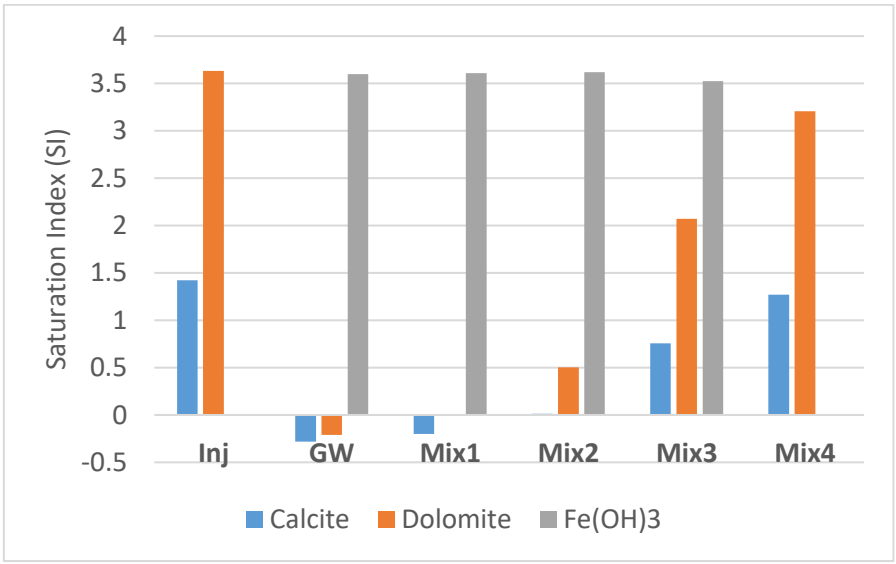

Figure 4: BH4165 *- saturation indices for calcite, dolomite and amorphous iron hydroxide. Mixing proportions: Mix1 = 80% GW:20% Injection; Mix2 = 60% GW:40% Injection; Mix3 = 40% GW:60% Injection; Mix4 = 20% GW:80% Injection. Calculated with* ***injection water analysis 2*** *(Surface water sample August 2017)*

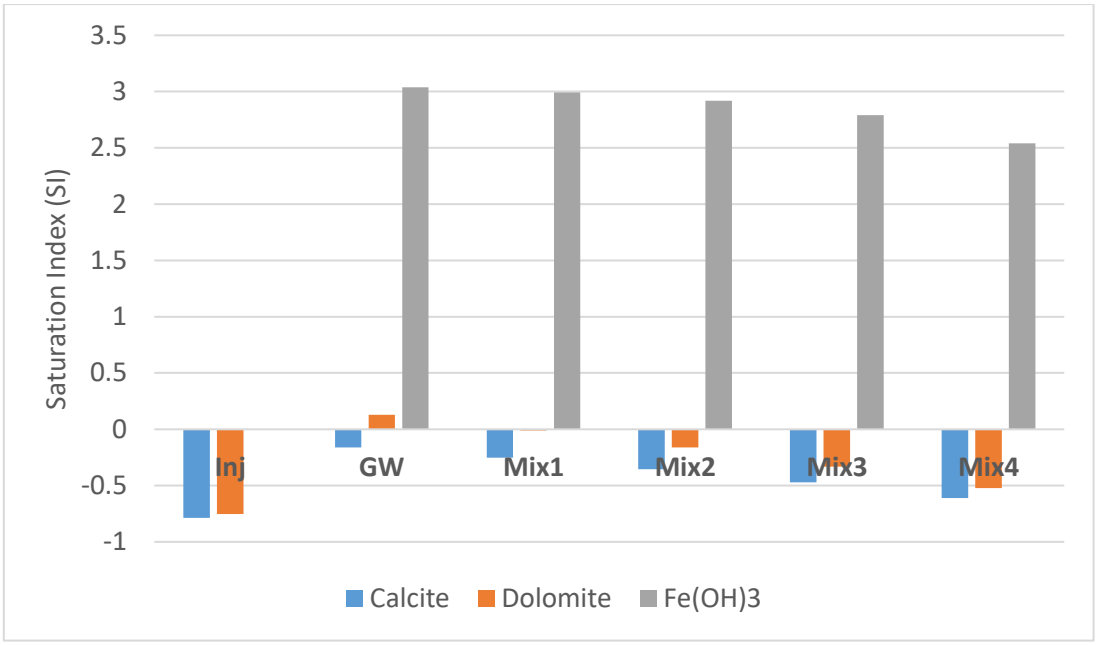

Figure 5: BH6501 *- saturation indices for calcite, dolomite and amorphous iron hydroxide. Mixing proportions: Mix1 = 80% GW:20% Injection; Mix2 = 60% GW:40% Injection; Mix3 = 40% GW:60% Injection; Mix4 = 20% GW:80% Injection. Calculated with* ***injection water analysis 1*** *(Surface water sample July 2017)*

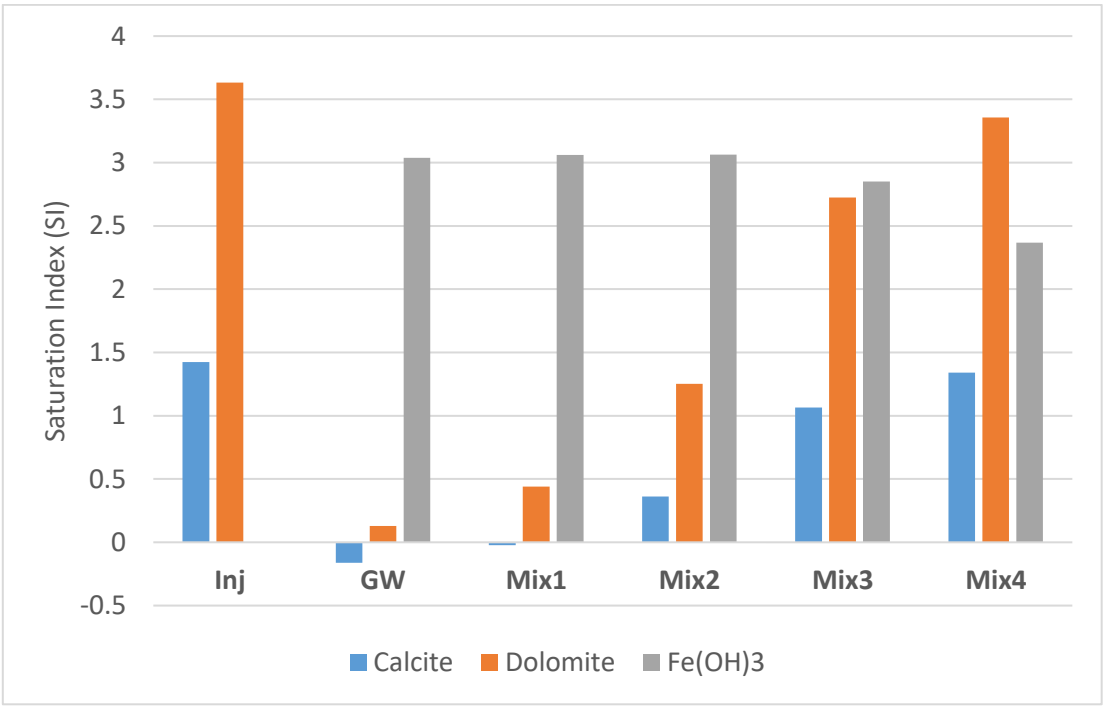

Figure 6: BH6501 *- saturation indices for calcite, dolomite and amorphous iron hydroxide. Mixing proportions: Mix1 = 80% GW:20% Injection; Mix2 = 60% GW:40% Injection; Mix3 = 40% GW:60% Injection; Mix4 = 20% GW:80% Injection. Calculated with* ***injection water analysis 2*** *(surface water sample August 2017)*

*Table1: Selected elements and saturation indices of injection water, groundwater (**BH 4164 – Ramotswa centre**) and mixed water before and after equilibration with dolomite and amorphous iron hydroxide. Mix1: 80% GW:20% Injection; Mix2: 60% GW:40% Injection; Mix3: 40% GW:60% Injection; Mix4: 20% GW:80% Injection. Concentrations in mol/L.*

	Injection1	GW	Mix1	Eq1	Mix2	Eq2	Mix3	Eq3	Mix4	Eq4
pH	7.06	8	7.75	7.11	7.53	7.15	7.35	7.20	7.20	7.24
C(IV)	6.49E-03	8.86E-03	8.39E-03	7.57E-03	7.91E-03	7.40E-03	7.44E-03	7.22E-03	6.96E-03	7.04E-03
Ca	3.93E-04	1.37E-03	1.18E-03	7.68E-04	9.81E-04	7.22E-04	7.85E-04	6.75E-04	5.89E-04	6.26E-04
Mg	2.29E-03	3.54E-03	3.29E-03	2.88E-03	3.04E-03	2.78E-03	2.79E-03	2.68E-03	2.54E-03	2.58E-03
Fe(II)	0.00E+00	3.91E-17	7.19E-17	2.59E-17	1.15E-16	1.69E-17	1.38E-16	1.11E-17	1.09E-16	7.36E-18
Fe(III)	0.00E+00	1.08E-06	8.60E-07	2.83E-08	6.45E-07	2.40E-08	4.30E-07	2.04E-08	2.15E-07	1.72E-08
Mn(II)	0.00E+00	2.21E-05	1.78E-05	1.78E-05	1.33E-05	1.34E-05	8.90E-06	8.90E-06	4.45E-06	4.45E-06
Mn(III)	0.00E+00	1.24E-18	2.73E-18	1.74E-17	4.67E-18	1.33E-17	5.86E-18	8.81E-18	4.87E-18	4.28E-18
SI Calcite	-0.7864	0.8869	0.5498	-0.3419	0.2152	-0.3412	-0.1031	-0.3413	-0.4255	-0.3423
SI Dolomite	-0.7516	2.3128	1.6586	0	1.0199	0	0.4286	0	-0.1462	0
SI CO2 (g)	-1.5904	-2.3212	-2.1048	-1.5444	-1.9188	-1.5974	-1.7787	-1.6532	-1.6728	-1.7123
SI O2 (g)	-0.7	-1.3173	-1.1032	-1.1031	-0.9554	-0.9555	-0.849	-0.8491	-0.7667	-0.7666
SI Fe(OH)3		1.6872	1.6392	0	1.5404	0	1.3761	0	1.0776	0

*Table 2:Selected elements and saturation indices of injection water, groundwater (**BH 4164 – Ramotswa centre**) and mixed water before and after equilibration with dolomite and amorphous iron hydroxide. Mix1: 80% GW:20% Injection; Mix2: 60% GW:40% Injection; Mix3: 40% GW:60% Injection; Mix4: 20% GW:80% Injection. Concentrations in mol/L.*

	Injection2	GW	Mix1	Eq1	Mix2	Eq2	Mix3	Eq3	Mix4	Eq4
pH	9.67	7	7.16	7.14	7.47	7.45	8.35	8.37	9.14	9.15
C(IV)	3.59E-03	8.94E-03	7.87E-03	7.87E-03	6.80E-03	6.80E-03	5.73E-03	5.73E-03	4.66E-03	4.66E-03
Ca	4.61E-04	9.74E-04	8.71E-04	8.71E-04	7.69E-04	7.69E-04	6.66E-04	6.66E-04	5.63E-04	5.63E-04
Mg	2.09E-03	1.65E-03	1.73E-03	1.73E-03	1.82E-03	1.82E-03	1.91E-03	1.91E-03	2.00E-03	2.00E-03
Fe(II)	0.00E+00	3.30E-13	9.77E-14	2.63E-17	1.89E-14	4.91E-18	2.99E-16	8.45E-20	4.81E-18	4.36E-21
Fe(III)	0.00E+00	1.41E-04	1.13E-04	2.82E-08	8.47E-05	2.06E-08	5.65E-05	1.69E-08	2.82E-05	2.70E-08
Mn(II)	0.00E+00	5.21E-06	4.17E-06	4.17E-06	3.12E-06	3.12E-06	1.71E-06	1.69E-06	4.76E-08	4.50E-08
Mn(III)	0.00E+00	3.85E-18	3.05E-18	3.23E-18	1.21E-18	1.28E-18	4.34E-20	4.05E-20	6.49E-23	5.83E-23
SI Calcite	1.4236	-0.28	-0.2009	-0.2242	0.0118	-0.0071	0.7558	0.7694	1.2709	1.2794
SI Dolomite	3.6325	-0.2093	0.0104	-0.0363	0.5024	0.4645	2.07	2.0974	3.2066	3.2243
SI CO2 (g)	-4.5422	-1.3713	-1.5708	-1.5521	-1.9182	-1.9012	-2.8635	-2.8782	-3.7878	-3.8011
SI O2 (g)	-0.7	-1.9464	-1.3093	-1.3093	-1.0542	-1.0542	-0.8994	-0.8995	-0.7889	-0.7889
SI Fe(OH)3		3.5977	3.6104	0	3.6191	0	3.5254	0	3.0259	0

*Table 3: Selected elements and saturation indices of injection water, groundwater (**BH 4165 – Ramotswa north**) and mixed water before and after equilibration with amorphous iron hydroxide. Mix1: 80% GW:20% Injection; Mix2: 60% GW:40% Injection; Mix3: 40% GW:60% Injection; Mix4: 20% GW:80% Injection. Concentrations in mol/L.*

	Injection1	GW	Mix1	Eq1	Mix2	Eq2	Mix3	Eq3	Mix4	Eq4
pH	7.06	7.00	7.01	6.99	7.02	7.01	7.03	7.02	7.05	7.04
C(IV)	6.49E-03	8.94E-03	8.45E-03	8.45E-03	7.96E-03	7.96E-03	7.47E-03	7.47E-03	6.98E-03	6.98E-03
Ca	3.93E-04	9.74E-04	8.58E-04	8.58E-04	7.42E-04	7.42E-04	6.25E-04	6.25E-04	5.09E-04	5.09E-04
Mg	2.29E-03	1.65E-03	1.78E-03	1.78E-03	1.91E-03	1.91E-03	2.03E-03	2.03E-03	2.16E-03	2.16E-03
Fe(II)	0.00E+00	3.30E-13	1.68E-13	5.06E-17	1.00E-13	3.46E-17	5.58E-14	2.49E-17	2.39E-14	1.82E-17
Fe(III)	0.00E+00	1.41E-04	1.13E-04	3.19E-08	8.47E-05	2.79E-08	5.65E-05	2.42E-08	2.82E-05	2.10E-08
Mn(II)	0.00E+00	5.21E-06	4.17E-06	4.17E-06	3.13E-06	3.13E-06	2.08E-06	2.08E-06	1.04E-06	1.04E-06
Mn(III)	0.00E+00	3.85E-18	4.57E-18	4.81E-18	4.07E-18	4.23E-18	3.03E-18	3.12E-18	1.65E-18	1.68E-18
SI Calcite	-0.7864	-0.28	-0.356	-0.378	-0.4409	-0.4586	-0.5372	-0.5501	-0.6497	-0.6567
SI Dolomite	-0.7516	-0.2093	-0.2861	-0.3301	-0.3751	-0.4107	-0.4788	-0.5046	-0.6017	-0.6157
SI CO2 (g)	-1.5904	-1.3713	-1.4106	-1.3945	-1.4519	-1.4388	-1.4954	-1.4859	-1.5414	-1.5362
SI O2 (g)	-0.7	-1.9464	-1.3029	-1.3029	-1.0489	-1.0489	-0.8945	-0.8945	-0.7846	-0.7846
SI Fe(OH)3		3.5977	3.5578	0	3.4906	0	3.3728	0	3.1309	0

*Table 4: Selected elements and saturation indices of injection water, groundwater (**BH 4165 – Ramotswa north**) and mixed water before and after equilibration with amorphous iron hydroxide. Mix1: 80% GW:20% Injection; Mix2: 60% GW:40% Injection; Mix3: 40% GW:60% Injection; Mix4: 20% GW:80% Injection. Concentrations in mol/L.*

	Injection2	GW	Mix1	Eq1	Mix2	Eq2	Mix3	Eq3	Mix4	Eq4
pH	9.67	7.00	7.16	7.14	7.47	7.45	8.35	8.37	9.14	9.15
C(IV)	3.59E-03	8.94E-03	7.87E-03	7.87E-03	6.80E-03	6.80E-03	5.73E-03	5.73E-03	4.66E-03	4.66E-03
Ca	4.61E-04	9.74E-04	8.71E-04	8.71E-04	7.69E-04	7.69E-04	6.66E-04	6.66E-04	5.63E-04	5.63E-04
Mg	2.09E-03	1.65E-03	1.73E-03	1.73E-03	1.82E-03	1.82E-03	1.91E-03	1.91E-03	2.00E-03	2.00E-03
Fe(II)	0.00E+00	3.30E-13	9.77E-14	2.63E-17	1.89E-14	4.91E-18	2.99E-16	8.45E-20	4.81E-18	4.36E-21
Fe(III)	0.00E+00	1.41E-04	1.13E-04	2.82E-08	8.47E-05	2.06E-08	5.65E-05	1.69E-08	2.82E-05	2.70E-08
Mn(II)	0.00E+00	5.21E-06	4.17E-06	4.17E-06	3.12E-06	3.12E-06	1.71E-06	1.69E-06	4.76E-08	4.50E-08
Mn(III)	0.00E+00	3.85E-18	3.05E-18	3.23E-18	1.21E-18	1.28E-18	4.34E-20	4.05E-20	6.49E-23	5.83E-23
SI Calcite	1.4236	-0.28	-0.2009	-0.2242	0.0118	-0.0071	0.7558	0.7694	1.2709	1.2794
SI Dolomite	3.6325	-0.2093	0.0104	-0.0363	0.5024	0.4645	2.07	2.0974	3.2066	3.2243
SI CO2 (g)	-4.5422	-1.3713	-1.5708	-1.5521	-1.9182	-1.9012	-2.8635	-2.8782	-3.7878	-3.8011
SI O2 (g)	-0.7	-1.9464	-1.3093	-1.3093	-1.0542	-1.0542	-0.8994	-0.8995	-0.7889	-0.7889
SI Fe(OH)3		3.5977	3.6104	0	3.6191	0	3.5254	0	3.0259	0

*Table 5: Selected elements and saturation indices of injection water, groundwater (**BH 6501 – Ramotswa south**) and mixed water before and after equilibration with amorphous iron hydroxide. Mix1: 80% GW:20% Injection; Mix2: 60% GW:40% Injection; Mix3: 40% GW:60% Injection; Mix4: 20% GW:80% Injection. Concentrations in mol/L.*

	Injection1	GW	Mix1	Eq1	Mix2	Eq2	Mix3	Eq3	Mix4	Eq4
pH	7.06	7.11	7.10	7.10	7.09	7.09	7.08	7.08	7.07	7.07
C(IV)	6.49E-03	7.69E-03	7.45E-03	7.45E-03	7.21E-03	7.21E-03	6.97E-03	6.97E-03	6.73E-03	6.73E-03
Ca	3.93E-04	1.14E-03	9.87E-04	9.87E-04	8.39E-04	8.39E-04	6.90E-04	6.90E-04	5.42E-04	5.42E-04
Mg	2.29E-03	2.42E-03	2.40E-03	2.40E-03	2.37E-03	2.37E-03	2.35E-03	2.35E-03	2.32E-03	2.32E-03
Fe(II)	0.00E+00	3.86E-14	2.69E-14	2.81E-17	1.84E-14	2.27E-17	1.14E-14	1.87E-17	5.40E-15	1.57E-17
Fe(III)	0.00E+00	3.53E-05	2.83E-05	2.89E-08	2.12E-05	2.57E-08	1.41E-05	2.29E-08	7.06E-06	2.04E-08
Mn(II)	0.00E+00	7.70E-06	6.16E-06	6.16E-06	4.62E-06	4.62E-06	3.08E-06	3.08E-06	1.54E-06	1.54E-06
Mn(III)	0.00E+00	6.27E-18	6.13E-18	6.22E-18	5.39E-18	5.45E-18	4.12E-18	4.15E-18	2.33E-18	2.34E-18
SI Calcite	-0.7864	-0.1608	-0.2525	-0.2587	-0.3551	-0.36	-0.4726	-0.4761	-0.6119	-0.6137
SI Dolomite	-0.7516	0.1298	-0.0098	-0.0224	-0.1619	-0.1718	-0.3305	-0.3374	-0.5226	-0.5262
SI CO2 (g)	-1.5904	-1.5319	-1.5436	-1.5387	-1.5553	-1.5515	-1.567	-1.5643	-1.5787	-1.5773
SI O2 (g)	-0.7	-1.3391	-1.1137	-1.1137	-0.9609	-0.9609	-0.8518	-0.8518	-0.7678	-0.7678
SI Fe(OH)3		3.0384	2.992	0	2.9174	0	2.7912	0	2.5398	0

*Table 6: Selected elements and saturation indices of injection water, groundwater (**BH 6501 – Ramotswa south**) and mixed water before and after equilibration with amorphous iron hydroxide. Mix1: 80% GW:20% Injection; Mix2: 60% GW:40% Injection; Mix3: 40% GW:60% Injection; Mix4: 20% GW:80% Injection. Concentrations in mol/L.*

	Injection2	GW	Mix1	Eq1	Mix2	Eq2	Mix3	Eq3	Mix4	Eq4
pH	9.67	7.11	7.33	7.33	7.82	7.81	8.70	8.70	9.23	9.24
C(IV)	3.59E-03	7.69E-03	6.87E-03	6.87E-03	6.05E-03	6.05E-03	5.23E-03	5.23E-03	4.41E-03	4.41E-03
Ca	4.61E-04	1.14E-03	1.00E-03	1.00E-03	8.66E-04	8.66E-04	7.31E-04	7.31E-04	5.96E-04	5.96E-04
Mg	2.09E-03	2.42E-03	2.36E-03	2.36E-03	2.29E-03	2.29E-03	2.22E-03	2.22E-03	2.15E-03	2.15E-03
Fe(II)	0.00E+00	3.86E-14	1.15E-14	1.03E-17	1.09E-15	9.57E-19	1.72E-17	2.38E-20	7.48E-19	3.17E-21
Fe(III)	0.00E+00	3.53E-05	2.83E-05	2.47E-08	2.12E-05	1.83E-08	1.41E-05	2.00E-08	7.06E-06	3.03E-08
Mn(II)	0.00E+00	7.70E-06	6.16E-06	6.16E-06	4.59E-06	4.59E-06	1.17E-06	1.15E-06	3.98E-08	3.92E-08
Mn(III)	0.00E+00	6.27E-18	3.32E-18	3.38E-18	6.97E-19	7.03E-19	8.51E-21	8.19E-21	3.89E-23	3.79E-23
SI Calcite	1.4236	-0.1608	-0.0224	-0.029	0.3628	0.36	1.0663	1.0709	1.3399	1.3419
SI Dolomite	3.6325	0.1298	0.4401	0.427	1.2527	1.2472	2.7234	2.7327	3.3565	3.3607

SI CO2 (g)	-4.5422	-1.5319	-1.7823	-1.7767	-2.3019	-2.2992	-3.2599	-3.2654	-3.9231	-3.9265
SI O2 (g)	-0.7	-1.3391	-1.1172	-1.1172	-0.9647	-0.9647	-0.8602	-0.8602	-0.7728	-0.7728
SI Fe(OH)3		3.0384	3.0598	0	3.0631	0	2.8509	0	2.3689	0